

# Light Water Reactor Sustainability Program

## Risk-Informed Analysis of Commercial Nuclear Reactors: the RISMC Approach and 10CFR50.69

D. Mandelli, C. Parisi, Z. Ma, D. Maljovec, A. Alfonsi, C. Smith



September 2017

DOE Office of Nuclear Energy

**DISCLAIMER**

This information was prepared as an account of work sponsored by an agency of the U.S. Government. Neither the U.S. Government nor any agency thereof, nor any of their employees, makes any warranty, expressed or implied, or assumes any legal liability or responsibility for the accuracy, completeness, or usefulness, of any information, apparatus, product, or process disclosed, or represents that its use would not infringe privately owned rights. References herein to any specific commercial product, process, or service by trade name, trade mark, manufacturer, or otherwise, does not necessarily constitute or imply its endorsement, recommendation, or favoring by the U.S. Government or any agency thereof. The views and opinions of authors expressed herein do not necessarily state or reflect those of the U.S. Government or any agency thereof.

# **Light Water Reactor Sustainability Program**

## **Risk-Informed Analysis of Commercial Nuclear Reactors: the RISMC Approach and 10CFR50.69**

**D. Mandelli, C. Parisi, Z. Ma, D. Maljovec, A. Alfonsi, C. Smith  
Idaho National Laboratory (INL)**

**September 2017**

**Idaho National Laboratory  
Idaho Falls, Idaho 83415**

**<http://www.inl.gov/lwrs>**

**Prepared for the  
U.S. Department of Energy  
Office of Nuclear Energy  
Under DOE Idaho Operations Office  
Contract DE-AC07-05ID14517**



## ABSTRACT

Probabilistic Risk Assessment (PRA) methods have been successfully employed in the nuclear industry in conjunction with deterministic analysis methods in order to assess risk associated to nuclear power plants. The final goal of these analyses is not only to determine frequency of core damage (or frequency of large release of radioactive material outside the containment) but also to determine what are the most probable accident sequences and the components that contribute the most to the overall plant risk. Following this reasoning the Nuclear Regulatory Commission (NRC) has released a rule, known as 10CFR50.69, that provides guidance to plant utilities to focus on the most critical (from a safety point of view) systems, structure and components (SSCs). The objective is to relax the quality requirements on the SSCs that do not significantly affect the plant risk and to identify SSCs that contribute the most to the plant safety. As of now, industry has started to address 10CFR50.69 by employing a blend of both deterministic and PRA methods with the objective to decrease plant operational costs while maintaining plant safety levels unchanged. In light of the limitations of classical PRA methods, (e.g., very conservative success criteria and large approximations on recovery actions) the RISMIC has developed a PRA method (which can be classified as dynamic PRA method) that employs system analysis codes (normally employed in deterministic safety analysis) coupled with statistical analysis codes. The driving advantage of this method is the much higher fidelity of the analysis since timing and sequencing of events are implicitly modeled, success criteria are defined on the plant dynamics and recovery actions are an integral part of the analysis. In this report, we show how 10CFR50.69 can be addressed by employing the RISMIC PRA method. We present the mathematical PRA framework behind 10CFR50.69 and how it can be extended to Dynamic PRA methods. We proved the soundness of the proposed method by employing it on standard reliability models and then on an industry relevant test case such as a large break Loss Of Coolant Accident (LOCA) scenario.

# CONTENTS

ABSTRACT.....	iii
FIGURES.....	v
TABLES.....	vi
ACRONYMS.....	vii
1. Introduction.....	1
1.1 Overview of 10CFR50.69.....	2
1.2 Summary of R&D Activities.....	3
2. The RISMC Approach.....	5
3. Measuring Risk Importance.....	7
3.1 Classical PRA Importance Metrics.....	7
3.2 Simulation-based PRA Importance Metrics.....	7
3.3 Potential Applications Within 10CFR50.69.....	12
4. Application: PWR LB-LOCA.....	13
4.1 Results.....	14
5. Conclusions.....	18
5.1 Publications.....	18
6. REFERENCES.....	19
APPENDIX A.....	21
APPENDIX B.....	22

## FIGURES

Figure 1. Example of system analysis using a combination FTs and ETs.....	1
Figure 2. Categorization of SSCs according to NRC rule 10CFR50.69.....	3
Figure 3. Overview of the RISMCM modeling approach.....	5
Figure 4. Relationship between simulator physics code (H) and control logic (C).....	6
Figure 5. Treatment of discrete (top) and continuous (bottom) stochastic variables for reliability purposes.....	9
Figure 6. Plot of a hypothetical pdfo(T) .....	10
Figure 7. Plot of margino for the case shown in Figure 2 .....	11
Figure 8. Plot of the pdfs for PCT (green) and CFT (red).....	11
Figure 9. Plot of the pdf of the variable CFT-PCT (left) and plot of the pdf of the margin, i.e., CFT-PCT > 0 (right). .....	12
Figure 10. PWR scheme. ....	13
Figure 11. PWR LB-LOCA analysis overview. ....	14
Figure 12. Branch probability comparison. ....	15
Figure 13. Histogram of PCT for the simulation belonging to branch 4 (see Figure 12).....	15
Figure 14. Updated ET structure given RELAP5-3D/RAVEN analysis. ....	16
Figure 15. LBLOCA DEGB cases. PCT (left), RPV level (right).....	17

## TABLES

Table 1. LBLOCA DEGB results.....	16
-----------------------------------	----



## ACRONYMS

ACC	Accumulator system
CD	Core Damage
CS	Containment Spray
DOE	Department of Energy
ECCS	Emergency Core Cooling System
EDG	Emergency Diesel Generator
EPRI	Electric Power Research Institute
ET	Event-Tree
FT	Fault-Tree
FV	Fusel-Vessely
INL	Idaho National Laboratory
LB-LOCA	Large Break LOCA
LOCA	Loss Of Coolant Accident
LPI	Low Pressure Injection system
LPR	Low Pressure Recirculation system
LWRS	Light Water Reactor Sustainability
MC	Monte-Carlo
NPP	Nuclear Power Plant
NRC	Nuclear Regulatory Commission
PCT	Peak Clad Temperature
PRA	Probabilistic Risk Assessment
PWR	Pressurized Water Reactor
pdf	Probabilistic Distribution Function
R&D	Research and Development
RAVEN	Risk Analysis Virtual ENvironment
RAW	Risk Achievement Worth
RIM	Risk Importance Measure
RRW	Risk Reduction Worth
RISC	Risk Informed Safety Class
RISMC	Risk-Informed Safety Margin Characterization
ROM	Reduced Order Model
RPV	Reactor Pressure Vessel
RRW	Risk Reduction Worth
RWST	Reactor Water Storage Tank
SG	Steam Generator
SI	Safety Injection

SR Safety Related  
SSCs Systems , Structures and Components

# Risk-Informed Analysis of Commercial Nuclear Reactors: the RISMC Approach and 10CFR50.69

## 1. INTRODUCTION

Safety and risk associated to nuclear power plants are typically measured by employing Probabilistic Risk Assessment (PRA) methods in conjunction with deterministic analysis methods. Deterministic methods employ system analysis codes (e.g., RELAP5 [1] or MELCOR [2]) in order to assure that plant safety systems can prevent Core Damage (CD) condition for a given set of accident conditions. PRA methods [3] employ static Boolean logic structures (Event Trees – FT – and Fault-Tree – FT –) in order to determine accident sequences that includes failure of System Structure and Components (SSCs) given a set of prescribed initiating events.

The goal of PRA methods is not only to determine frequency of CD (or frequency of large release of radioactive material outside the containment or early cancer fatalities) but also to determine what are the most probable accident sequences and the components that contribute the most to the overall plant risk.

This is performed by modeling deductively the accident progression using ET structures and by modeling inductively the stochastic failure of the safety systems using FT structures. Figure 1 shows a simplified ET for a large break loss of cooling accident (LOCA). In order to reach a safe state of the plant, the reactor protection system trips the reactor and performs the cooling of the reactor through the emergency cooling system (ECCS). A failure in any of these two systems will cause CD. Note that in the ET pictured in Figure 1, the sequencing of events (and accompanying branching conditions) are already pre-fixed in the system logic designed by the analyst.

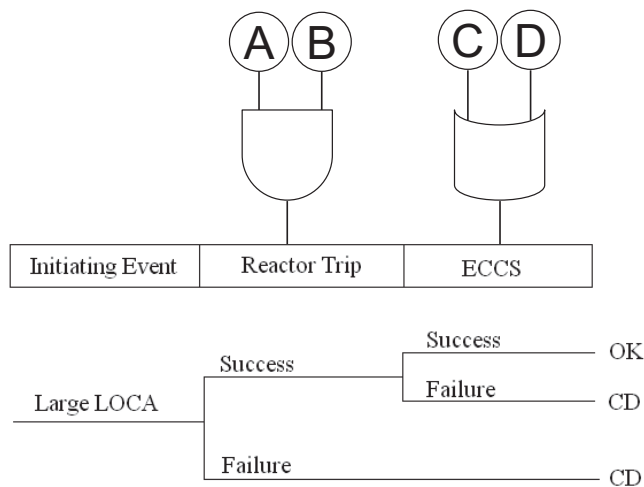


**Figure 1. Example of system analysis using a combination FTs and ETs.**

Branching probabilities associated to Reactor Trip and ECCS are determined using FTs: a combinations of logic gates (e.g., AND and OR gates) which connect basic events (i.e., A, B, C and D) to the Top Event (e.g., failure of ECCS). For the system pictured in Figure 1, the reactor trip system can fail if both events A and B occur (“AND” gate) while ECCS system fails if either events C or D occur (“OR” gate)

In light of the limitations of classical PRA methods (e.g., very conservative success criteria and large approximations on recovery actions) the RISMC project [4] has developed a PRA method (which can be classified as dynamic PRA method) that employs system analysis codes (normally employed in deterministic safety analysis) coupled with statistical analysis codes. The driving advantage of this method is the much higher fidelity of the analysis since timing and sequencing of events are implicitly modeled, success criteria are defined on the plant dynamics and recovery actions are integral part of the analysis.

In early 2000, the Nuclear Regulatory Commission (NRC) released a rule, known as 10CFR50.69, that provides guidance to plant utilities and operators to focus on the most critical (from a safety point of view) systems, structures and components (SSCs). The objective is to relax the quality requirements (and, thus, decrease procurement costs) on the SSCs that do not significantly affect the plant risk and to identify SSCs that actually contribute the most to the plant safety. As of now, industry has started to address 10CFR50.69 by employing a blend of both deterministic and PRA methods with the objective to decrease plant operational costs while maintaining plant safety levels unchanged.

The essential step behind 10CFR50.69 is to measure risk importance of SSCs [5]: this is usually performed using classical Risk Importance Measures (RIMs) such as Risk Achievement Worth (RAW) and Fussler-Vessely (FV) applied to the data generated ET-FT methods (i.e., cut sets).

In this report we show how 10CFR50.69 can be addressed by employing the RISMC PRA method. Firstly, we present the mathematical PRA framework behind measuring risk importance of SSCs and how it can be extended to Dynamic PRA methods. We proved the soundness of the proposed method by employing it on standard reliability models and then on an industry relevant test case such as a Large Break Loss Of Coolant Accident (LOCA) scenario.

## **1.1 Overview of 10CFR50.69**

In early 2000s, the US Nuclear Regulatory Commission (NRC) released the 10CFR50.69 [6] rule which contains categorization requirements for plant SSCs supported by a regulatory guide. Additionally, the rule contains a new treatment requirements that applies to SSCs based on their associated risk-informed safety class (RISC) categorization. This rule has the benefit of grouping and integrating all the risk-informed requirements into one single rule.

The rule approach enables the NRC to identify in one place what the regulatory treatment Safety-related SSCs that a risk-informed categorization process determines are significant contributors to plant safety are termed RISC-1 SSCs (see Figure 2). Non safety-related SSCs that the risk-informed categorization determines to be significant contributors to plant safety are termed RISC-2 SSCs. Safety-related SSCs that a risk-informed categorization process determines are not significant contributors are termed RISC-3 SSCs. Finally, non safety-related SSCs that a risk-informed categorization process determines are not significant contributors to plant safety are termed RISC-4 SSCs.

RISC-1 and RISC-2 SSCs will continue to meet applicable special treatment requirements and will also have requirements that ensure that key categorization assumptions that relate to credited performance in beyond design basis scenarios are technically valid, and updated consistent with the process feedback requirements in the rule. RISC-3 SSCs will have requirements that maintain with reasonable confidence the capability of performing their safety-related functions under design basis conditions.

RISC-4 SSCs will be removed from any applicable special treatment requirements and have no additional requirements imposed by 10CFR50.69 rule (recognizing that any technical/functional requirements continue to apply unless they are changed via the normal design change process including 10CFR50.69 rule).

As part of the “Delivering the Nuclear Promise”, the Nuclear Energy Institute (NEI) in collaboration with Electric Power Research Institute (EPRI) started a set of operational activities to assist the nuclear industry with the goals of:

- Maintain Operational record: safety remains an essential priority, advanced reliability and resilience of plants
- Increase value: clean energy benefits, R&D improvements
- Improve efficiency: reduced operation costs, maintain/increase capacity factor

The last goal (i.e., the reduction of operational costs) is being addressed by extensively employing the 10CFR50.69 rule for a large number of plant systems.

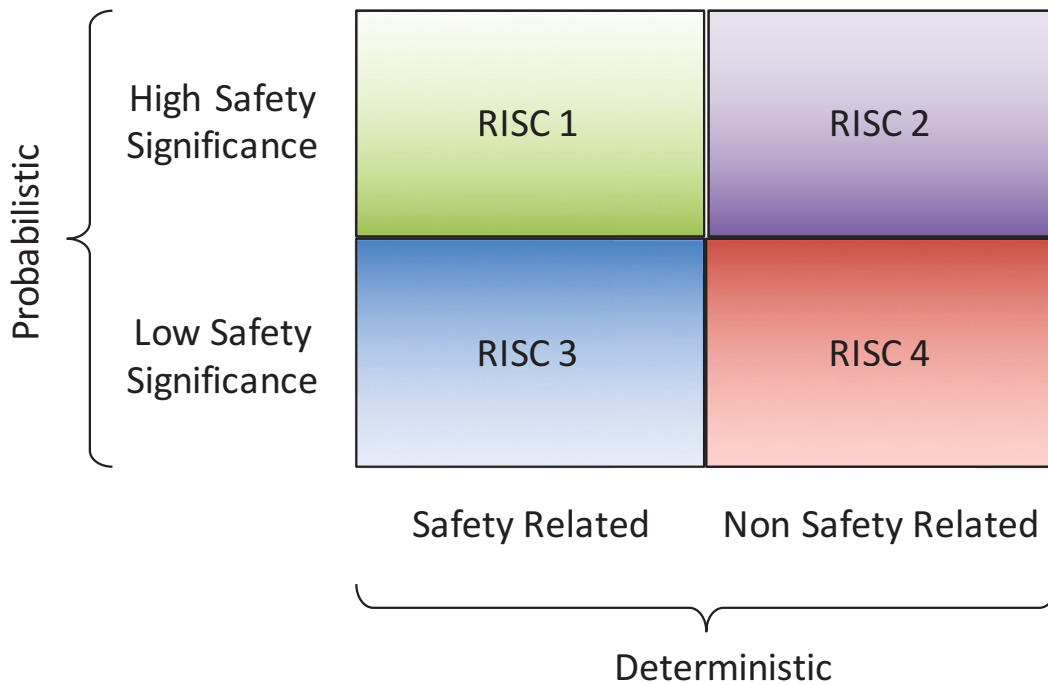


**Figure 2. Categorization of SSCs according to NRC rule 10CFR50.69.**

## 1.2 Summary of R&D Activities

During FY17, as part of this R&D project, we have performed the following activities in order to address 10CFR50.69 using the RISM approach:

1. Development of RIMs for any data generated by simulation-based (i.e., dynamic) PRA method such as Monte-Carlo [7] or Dynamic Event Trees (DETs) [8]
2. Implementation of these RIMs as integral part of the RAVEN statistical framework
3. Extension of these RIMs on a time dependent domain which can be used as part of risk-monitoring tools

4. Validation of the proposed RIMs against analytical test cases and against classical PRA tools such as SAPHIRE
5. Performed a full simulation based PRA analysis for an industry level test case such as PWR LB-LOCA
6. Comparison of the analysis between RAVEN-RELAP5 and SAPHIRE on the PWR LB-LOCA test case
7. Development of new margin-centric RIMs that incorporate in the assessment the intrinsic dynamic behavior of accident progression

## 2. THE RISMIC APPROACH

The RISMIC approach employs both deterministic and stochastic methods in a single analysis framework (see Figure 3). In the deterministic method set we include:

- Modeling of the thermal-hydraulic behavior of the plant [9]
- Modeling of external events such as flooding [10]
- Modeling of the operator responses to the accident scenario [11]

Note that deterministic modeling of the plant or external events can be performed by employing specific simulator codes but also surrogate models [12], known as reduced order models (ROM). ROMs would be employed in order to decrease the high computational costs of codes. In addition, *multi-fidelity codes* can be employed to model the same system; the idea is to switch from low-fidelity to high-fidelity code when higher accuracy is needed (e.g., use low-fidelity codes for steady-state conditions and high-fidelity code for transient conditions)

In the stochastic modelling we include all stochastic parameters that are of interest in the PRA analysis such as:

- Uncertain parameters
- Stochastic failure of system/components

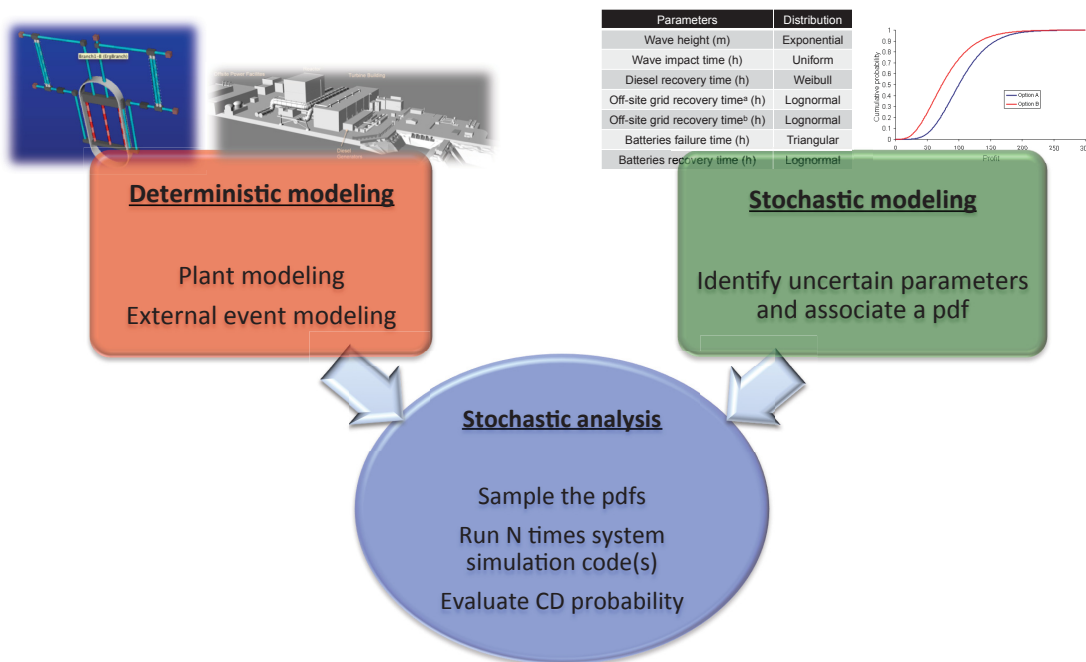


Figure 3. Overview of the RISMIC modeling approach.

The RISMIC approach heavily relies on multi-physics system simulator codes (e.g., RELAP5-3D [1]) coupled with stochastic analysis tools (e.g., RAVEN [13,14]). From a PRA point of view, a simulation run can be described by using two sets of variables:

- $\mathbf{c} = \mathbf{c}(t)$  represents the status of components and systems of the simulator (e.g., status of emergency core cooling system, AC system)

- $\theta = \theta(t)$  represents the temporal evolution of a simulated accident scenario, i.e.,  $\theta(t)$  represents a single simulation run. Each element of  $\theta$  can be for example the values of temperature or pressure in a specific node of the simulator nodalization.

From a mathematical point of view, a single simulator run can be represented as a single trajectory in the phase space. The evolution of such a trajectory in the phase space can be described as follows:

$$\begin{cases} \frac{\partial \theta(t)}{\partial t} = \mathcal{H}(\theta, \mathbf{s}, \mathbf{c}, t) \\ \frac{\partial \mathbf{c}(t)}{\partial t} = \mathcal{C}(\theta, \mathbf{s}, \mathbf{c}, t) \end{cases} \quad (1)$$

where:

- $\mathcal{H}$  is the actual simulator code that describes how  $\theta$  evolves in time
- $\mathcal{C}$  is the operator which describes how  $\mathbf{c}$  evolves in time, i.e., the status of components and systems at each time step
- $\mathbf{s}$  is the set of stochastic parameters

Starting from the system located in an initial state,  $\theta(t = 0) = \theta(0)$ , and the set of stochastic parameter values (which are generally generated through a stochastic sampling process), the simulator determines at each time step the temporal evolution of  $\theta(t)$ . At the same time, the system control logic<sup>1</sup> determines the status of the system and components  $\mathbf{c}(t)$ . The coupling between these two sets of variables is shown in Figure 4.

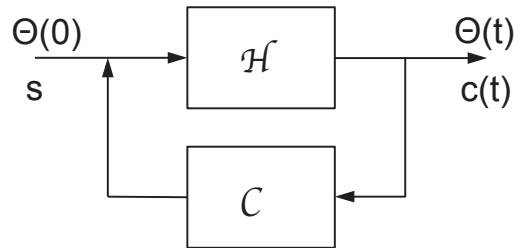


**Figure 4. Relationship between simulator physics code (H) and control logic (C).**

By using the RISMC approach, the PRA analysis is performed by [15]:

1. Associating a probabilistic distribution function (pdf) to the set of stochastic parameters  $\mathbf{s}$  (e.g., timing of events)
2. Performing stochastic sampling of the pdfs defined in Step 1
3. Performing a simulation run given  $\mathbf{s}$  sampled in Step 2, i.e., solve the system of equations (1)
4. Repeating Steps 2 and 3  $M$  times and evaluating user defined stochastic parameters such as CD probability ( $P_{CD}$ ).

The goal of RIM analysis is to measure risk importance of the set of stochastic parameters  $\mathbf{s}$ . The analysis presented in this report focuses on how RIMs can be extended to Dynamic PRA data.

---

<sup>1</sup> Which is usually an integral part of the system simulator



### 3. MEASURING RISK IMPORTANCE

The value of a PRA analysis is not limited to the determination of the risk associated to a nuclear power plant (through the determination of CD or LERF probability) but, more importantly, it provides insights about which components/systems impact the most the plant risk and which ones are the most safety relevant (i.e., they assure plant basic safety functions).

These insights can be generated by defining a set of metrics that measure the risk importance of system/components. Typically, in classical PRA methods, the set of metrics are determined by evaluating CD probability assuming the component failed or perfectly reliable (see Section 3.1).

#### 3.1 Classical PRA Importance Metrics

In ET-FT based PRA methods, for any basic event, the most used RIMs measures are: Risk Achievement Worth (RAW), Risk Reduction Worth (RRW), Birnbaum (B) and Fussell-Vesely (FV) [5,16]. All these RIMs are calculated by determining three values based on core damage frequency (CDF):

- $R_o$ : nominal CDF
- $R_i^-$ : CDF for basic event  $i$  assuming perfectly reliable
- $R_i^+$ : CDF for basic event  $i$  assuming it has failed

Once these three values are determined, then the RIMs are calculated [5] as follows for each basic event  $i$ :

$$RAW_i = \frac{R_i^+}{R_o} \quad (1)$$

$$RRW_i = \frac{R_o}{R_i^-} \quad (2)$$

$$B_i = R_i^+ - R_i^- \quad (3)$$

$$FV_i = \frac{R_o - R_i^-}{R_o} \quad (4)$$

Note the four RIMs listed above is not exhaustive; in literature, it is possible to find additional RIMs such as the Differential Importance Measure (DIM) [17]. Since, the scope of this paper is limited to risk-informed application of 10CFR50.69, we focused this report only on the four RIMs listed above.

#### 3.2 Simulation-based PRA Importance Metrics

In a Dynamic PRA environment,  $R_o$  is obtained (e.g., through Monte-Carlo sampling) by:

- Running  $N$  simulations (e.g., RELAP5-3D runs)
- Counting the number  $N_{CD}$  of simulations that lead to core damage (CD) condition
- Calculating  $R_o = \frac{N_{CD}}{N}$

Note that while basic events in classical PRA are mainly Boolean, in a Dynamic PRA environment the sample parameters can be, not only Boolean, but more often continuous. In this work we assume that basic events in a classical PRA framework coincide with the stochastic parameters in a RISM framework.

As an example, let us consider two basic events:

1. Emergency Diesel Generator (EDG) failure to start, and,
2. EDG failure to run

In classical PRA analysis, a probability value is associated to both basic events. On the other side, in a Dynamic PRA framework, a Bernoulli distribution could be associated to the first basic event and a continuous distribution (e.g., exponential distribution) could be associated to the second basic event.

At this point a challenge arises: the determination of  $R_i^-$  and  $R_i^+$  for each sampled parameter; two possible approaches can be followed<sup>2</sup>:

1. Perform a Dynamic PRA for  $R_o$  and for each  $R_i^-$  and  $R_i^+$
2. Determine an approximated value of  $R_i^-$  and  $R_i^+$  from the simulation runs generated to calculate  $R_o$

Regarding Approach 1, given the computational costs of each Dynamic PRA, it is unfeasible to determine  $R_i^-$  and  $R_i^+$  for each sampled parameter. In fact, if we consider  $M$  sample parameters (i.e.,  $S$  basic events), then the risk importance analysis would require  $2S + 1$  Dynamic PRA analyses.

Regarding Approach 2, a method (implemented in RAVEN as an internal post-processor) was developed and it is here presented. This method requires an input from the user:

- Range,  $I_i^-$ , of the variable  $s_i$  that can be associated to “basic event with component perfectly reliable”
- Range,  $I_i^+$ , of the variable  $s_i$  that can be associated to “basic event in a failed status”

Given this kind of information, it is possible to calculate  $R_i^+$  and  $R_i^-$  as follows<sup>3</sup>:

$$R_o = \frac{N_{CD}}{N} \quad (6)$$

$$R_i^+ = \frac{N_{CD, s_i \in I_i^+}}{N} \quad (7)$$

$$R_i^- = \frac{N_{CD, s_i \in I_i^-}}{N} \quad (8)$$

Note that this approach has an issue related to the choices of  $I_i^+$  and  $I_i^-$ . Depending on their values,  $R_i^+$  and  $R_i^-$  might change accordingly. In addition, the statistical error associated to the estimates of  $R_i^+$  and  $R_i^-$  also changes.

An example is shown in Figure 5 for both cases (discrete and continuous) of a basic event  $x_i$  represented as a stochastic variable which is sampled (e.g., through a Monte-Carlo process) for each simulation run. Consider the continuous case and assume  $s_i$  correspond to the basic event “EDG failure to run”. The user might impose the following in order to determine  $R_i^+$  and  $R_i^-$ :

- $I_i^- = [T_i^-, \infty]$  where  $T_i^-$  may be set equal to the simulation mission time (e.g., 24 hours). This implies that a sampled value for EDG failure to run greater than 24 hours implies that the EDG actually does not fail to run (reliability equal to 1.0)
- $I_i^+ = [0, T_i^+]$  where  $T_i^+$  may be set to an arbitrary small value (e.g., 5 min). This implies that a sampled value for EDG failure to run smaller than 5 min implies a reliability equal to 0.0

Note that while the definition of  $I_i^-$  is perfectly reasonable, one would argue that a smaller interval should be chosen for  $I_i^+$  (e.g., 30 seconds or less).

<sup>2</sup> A possible approach would be to develop a new sampling strategy designed ad-hoc to maximize the amount of data that can be generated to determine more reliable values of  $R_i^-$  and  $R_i^+$ . However, research of effective algorithms is still under way.

<sup>3</sup> It is here indicated:

- $N_{CD, s_i \in I_i^+}$  as the number of simulations leading to core damage and with parameter  $s_i \in I_i^+$
- $N_{CD, s_i \in I_i^-}$  as the number of simulations leading to core damage and with parameter  $s_i \in I_i^-$

Recall that ideally, a value of  $s_i = 0.0$  should be theoretically chosen (and not an interval); however, given the nature of the distribution this is not allowed. Given the nature of the problem, we are bound to choose an interval  $I_i^+$ :

- A small interval in the neighbor of  $s_i = 0.0$  would lead to a value of  $R_i^+$  close to the theoretical one. However, the number of actual sampled values falling in  $I_i^+$  would be very small, i.e., large stochastic error.
- A large interval in the neighbor of  $s_i = 0.0$  would lead to a value of  $R_i^+$  far from the theoretical one. However, the number of actual sampled values falling in  $I_i^+$  would be very high, i.e., small stochastic error.

A solution to the large statistical error associated to a very small interval  $I_i^+$  can be solved by employing different sampling algorithms other than the classical Monte-Carlo one.

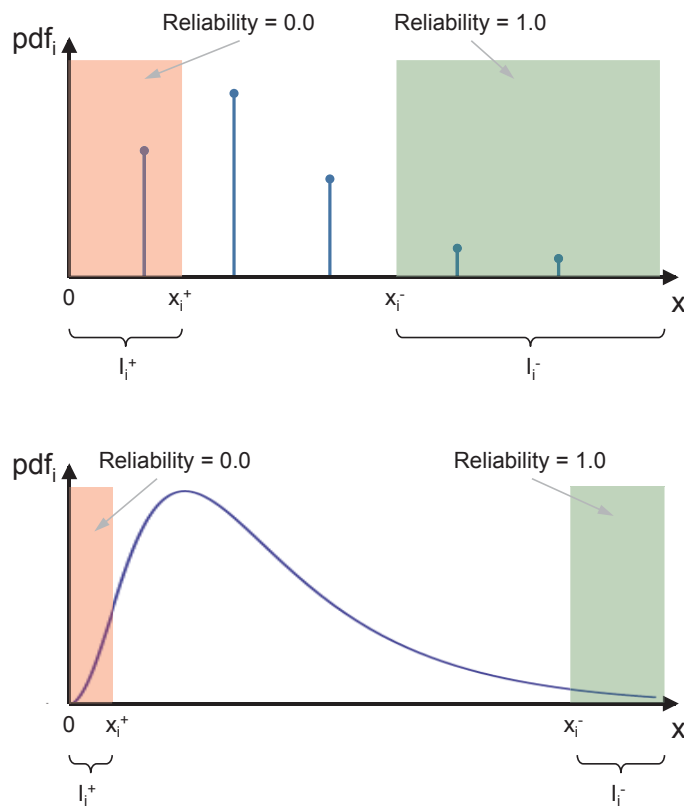


**Figure 5. Treatment of discrete (top) and continuous (bottom) stochastic variables for reliability purposes.**

As an example, a better resolution of the final value for  $R_i^+$  can be achieved by sampling uniformly the range of variability of  $x_i$  and associating an importance weight to each sample. At this point the counting variable  $N_{CD}$  is weighted by the weight of each sample. By sampling uniformly the range of variability of  $x_i$ , the number of samples in the interval  $I_i^+$  would be significantly higher.

Note that the RIMs described so far are limited to a binary logic of the outcome variable (e.g., OK vs. CD). Dynamic PRA approaches typically generate a continuous value of the outcome variables (e.g., Peak Clad Temperature - PCT). In our application (see previous sections) we typically convert PCT to a discrete one as follows:

- $PCT > 2200 F$ : outcome = CD

- $PCT < 2200$  F: outcome = OK

Given the different structure of the approach used in this paper to solve a PRA problem (i.e., Dynamic instead of classical PRA), the reader might think that a different set of RIMs should/could be developed in order to capture the nature of the problem solved using Dynamic PRA.

As a starting point, it would be worth investigating the nominal probabilistic distribution (pdf) of PCT with the one obtained when reliability of each basic event (sampled parameter) is 0.0 or 1.0. So now we can indicate:

1.  $pdf_o(T)$ : nominal pdf of PCT
2.  $pdf_i^-(T)$ : pdf of PCT associated to basic event  $i$  assuming basic event is perfectly reliable
3.  $pdf_i^+(T)$ : pdf of PCT associated to basic event  $i$  assuming basic event has failed

An example is shown below for a hypothetical case where obtained  $pdf_o(T)$  is indicated using an histogram while the limit value for PCT is shown using the red line passing at 2200 F.

In order to make a connection to what has been presented in the previous section, note that by looking at Figure 6:

$$R_o = \int_{2200}^{\infty} pdf_o(T) dT$$

As part of the RISMC analysis, the user might want to supplement the results obtained in the previous section with the information associated to a more effective margin analysis.

In particular, of interest for RISMC applications is (see Figure 7) the concept of margin:

$$margin = 2200 - PCT \text{ given } (PCT < 2200)$$

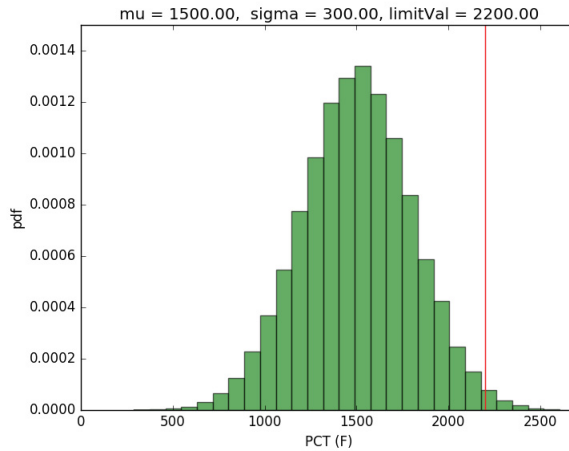


**Figure 6. Plot of a hypothetical  $pdf_o(T)$**

Using the same philosophy indicated in the previous section for classical RIMs, we want to determine:

1.  $margin_o$ : pdf of the variable  $2200 - PCT$  given that  $PCT < 2200$
2.  $margin_i^-$ : pdf of the variable  $2200 - PCT$  given that  $PCT < 2200$  for basic event  $i$  assuming it is perfectly reliable
3.  $margin_i^+$ : pdf of the variable  $2200 - PCT$  given that  $PCT < 2200$  for basic event  $i$  when its assumed to be failed

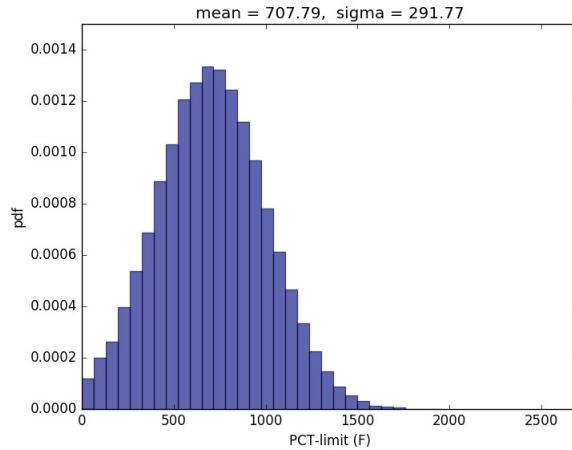


**Figure 7. Plot of  $margin_o$  for the case shown in Figure 2**

Note now that  $margin_o$ ,  $margin_i^-$  and  $margin_i^+$  are now pdfs and not numerical values. Hence, now the challenge arises on how to compare two pdfs:

- $margin_o$  vs.  $margin_i^-$
- $margin_o$  vs.  $margin_i^+$

A new definition of margin can be then defined:

$$margin = (CFT - PCT) \text{ given } (CFT - PCT > 0)$$

From here, once the pdf associated to the margin variable is determined it is possible to employ either the Z-tests or the Kolmogorov–Smirnov test in order to measure how this pdf changes when each basic event is considered perfectly reliable or failed.

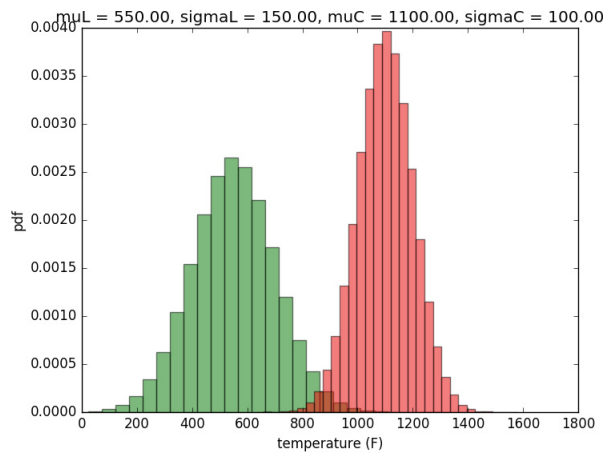


**Figure 8. Plot of the pdfs for PCT (green) and CFT (red).**

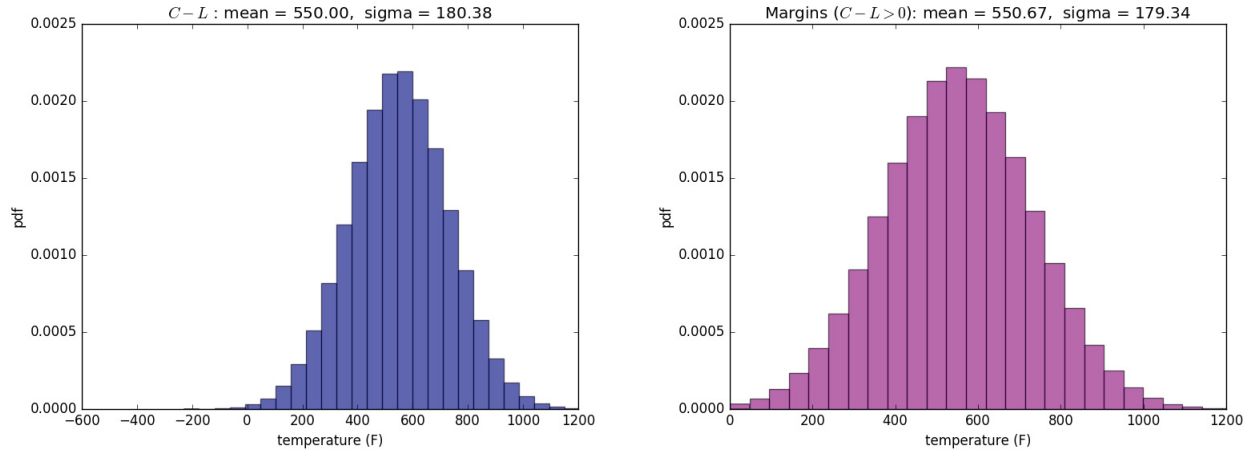


**Figure 9. Plot of the pdf of the variable  $CFT - PCT$  (left) and plot of the pdf of the margin, i.e.,  $CFT - PCT > 0$  (right).**

### 3.3 Potential Applications Within 10CFR50.69

The NRC rule 10CFR50.69 [6] provides guidance to identify components that are under strict quality assurance requirements and are minor contributors to the overall plant risk. Hence, an outcome of this rule is the reduction of plant operational costs while maintaining the same safety levels using risk-informed approaches.

In addition, the information generated by the RISMC tools can be employed to:

- Invest plant resources on the actual SSCs that guarantee plant safety
- Measure probabilistically the safety margins associated to safety related SSCs
- Optimize maintenance and testing procedures directed toward components and systems that guarantee plant safety during accident scenarios
- Provide insights to reactor operator crews about the components and systems that require constant monitoring during accident conditions
- Design recovery actions and quantify timing to perform such actions

## 4. APPLICATION: PWR LB-LOCA

In order to test the methods here proposed we have identified several analytical test cases based on classical reliability configurations (e.g., series/parallel, components in stand-by, K-out-of-N) and we have also developed additional test cases using industry PRA codes such SAPHIRE. For all cases, the obtained results were matching the analytical ones within the statistical error boundaries.

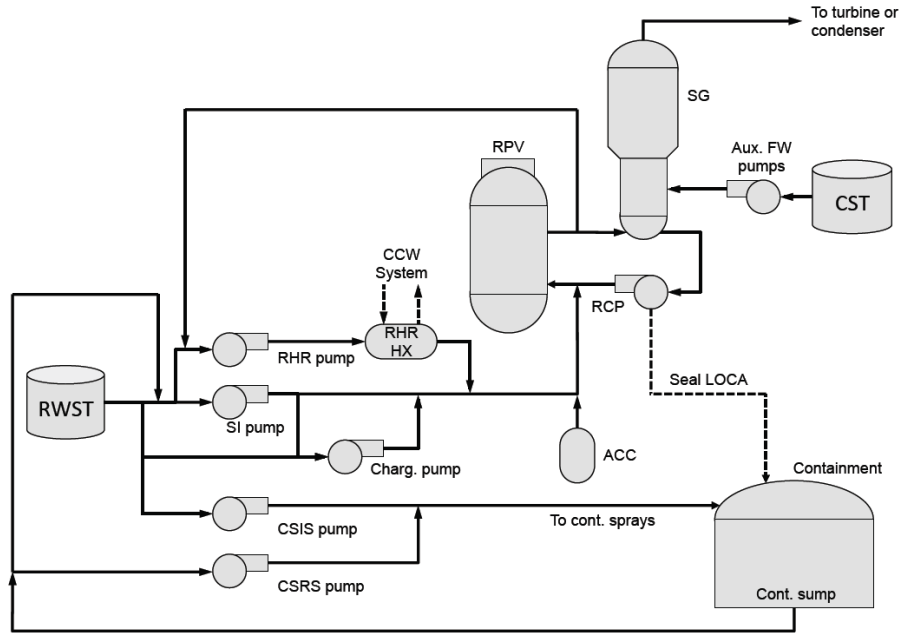


**Figure 10. PWR scheme.**

In addition, we have developed additional thorough benchmarking testing between our approach (using RAVEN/RELAP5-3D) and classical approach (using SAPHIRE) for a more relevant test case: a PWR LB-LOCA. The system considered is a 3-loop PWR system (see Figure 10) which undergoes a double guillotine break of one of the three hot-legs.

In this scenario, depressurization of the primary vessel occurs very quickly and large amount of water inventory is lost due to the break. In order to compensate loss of water inventory and provide cooling to the core in order to avoid core damage, several systems are employed:

- Accumulator system (ACC) which consists of water tanks that are employed right at the beginning of the transient in order to flood the RPV
- Low Pressure Injection (LPI) system which is an injection system that transfers cold water from the RWST tank to the RPV
- Low Pressure Recirculation (LPR) system which is employed once the RWST tank is empty; this system is still composed by the same components of the LPI system but water source is now the water collected inside the containment through the containment sump. Thus the water lost from the RPV is collected at the bottom of the containment, it is cooled down through heat-exchangers and it is injected back into the RPV (i.e., low pressure recirculation mode).
- Containment cooling system which controls containment thermodynamics behavior (temperature and pressure) in order to maintain its structural integrity

An overview of the performed analysis is shown in Figure 11 and it is structured as follows:

1. Simplify the structure of the LB-LOCA FTs of SAPHIRE by grouping its basic events into macro basic events.
2. Perform the calculation of the obtained SAPHIRE ET-FT model: determine CD probability, probability of each ET branch and the risk importance of each macro basic event
3. Consider the SAPHIRE ET for the LB-LOCA initiating event and model the RELAP5-3D accident progression following consistently with the SAPHIRE ET logic.
4. Construct the PWR logic based on the same macro basic events determined in Step 1: these macro basic events constitute the stochastic variables sampled by RAVEN
5. Perform a dynamic analysis using RAVEN/RELAP5-3D for the system constructed in Steps 3 and 4, and determine probability of each ET branch and the risk importance of each macro basic events
6. Compare the results obtained in Steps 3 and 5

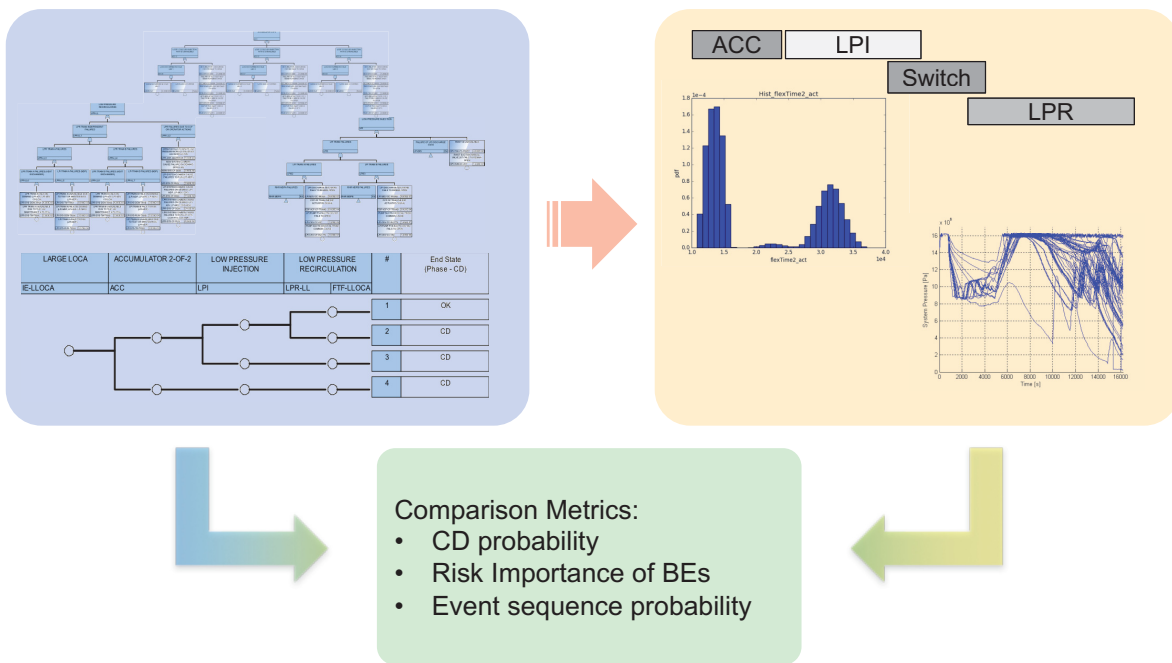


Figure 11. PWR LB-LOCA analysis overview.

## 4.1 Results

At a first glance, the two analyses provided almost identical results in terms of core damage probability:  $8.13 \text{ E-}3$  from SAPHIRE calculation and  $8.24 \text{ E-}3$  from RAVEN/RELAP5-3D. However, the first differences between the two methods arise when we evaluate the probability associated to each branch of the ET as indicated in Figure 12.

The first three branches have characterized with almost identical probabilities values; on the other side, probability of branch 4 had a much lower probability value when RAVEN/RELAP5-3D was employed:  $5.76 \text{ E-}10$ . The cause of this difference is the success criteria that in SAPHIRE requires 2 ACCs out of 2 while one ACC system (out of 2) is sufficient to avoid CD in the first seconds of the transient.



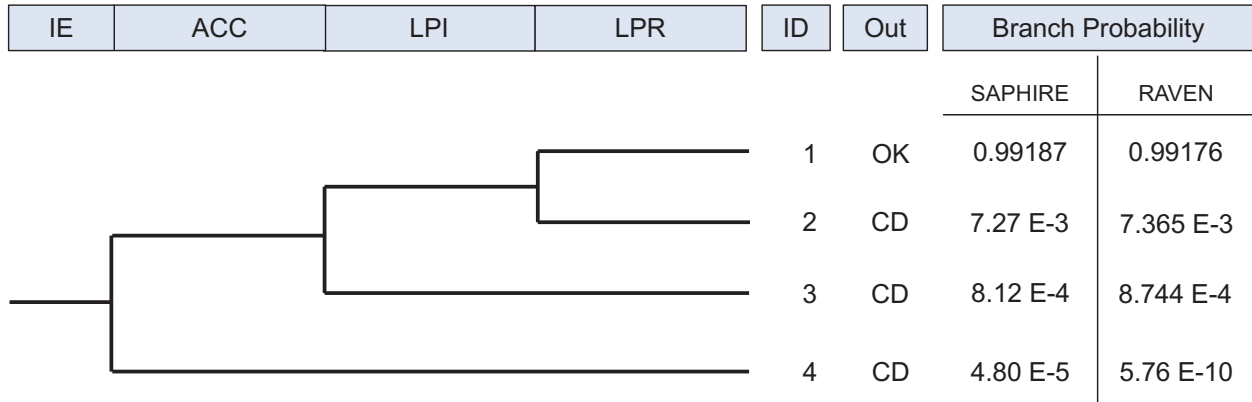


**Figure 12. Branch probability comparison.**

Given these differences, we have investigated the Peak Clad Temperature (PCT) for all simulations belonging to Branch 4. Figure 13 shows the histogram of PCT for all simulation falling in Branch 4: note that several simulations are not actually leading to CD condition. This implies that a failure of the ACC system does not imply CD. In fact, the LPI system can avoid CD if both ACCs have failed; depending on the number of LPI trains available the safety margin (i.e., 2200 - PCT) can range between 214 C and 422 C (see Figure 13).

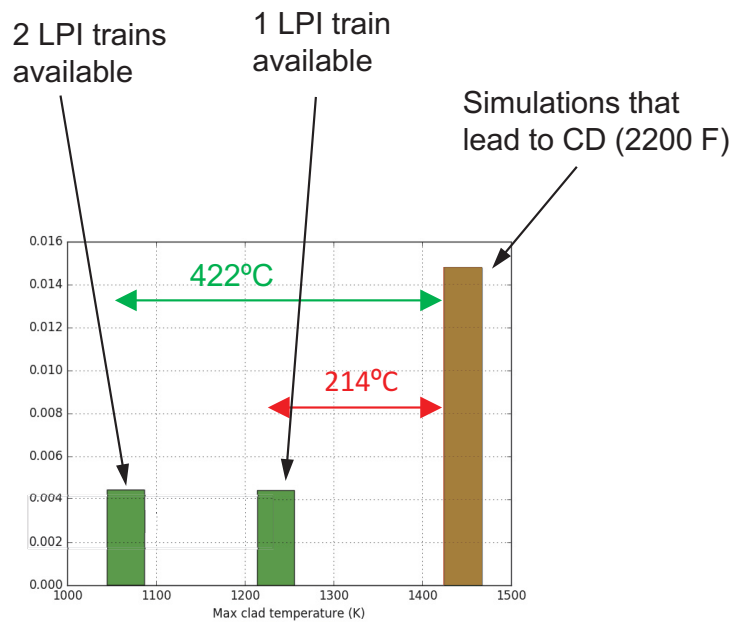


**Figure 13. Histogram of PCT for the simulation belonging to branch 4 (see Figure 12)**

Thus, from the RAVEN/RELAP5-3D analysis Branch 4 needs to be restructured to reflect these considerations (i.e., ACC failure does not imply CD condition). In this respect, Figure 14 shows the ET structure updated from the results generated by the RAVEN/RELAP5-3D analysis. Note that the additional branching conditions on LPI and LPR have been added (when ACC is assumed failed) and two additional ET branches have been added.

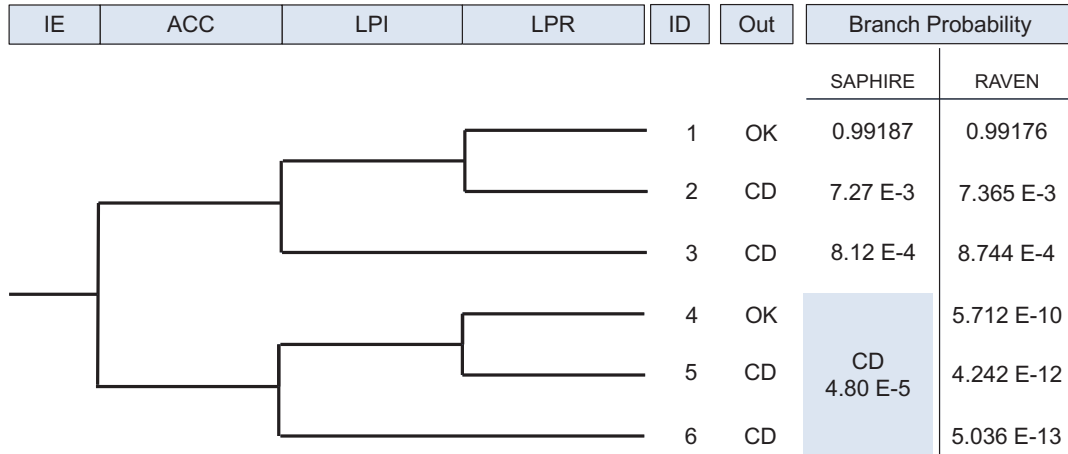


**Figure 14. Updated ET structure given RELAP5-3D/RAVEN analysis.**

This updated ET structure directly affected the RIM analysis: the RAW and FV importance measure of the basic events associated to LPI and LPR are identical between the two analyses. The only difference between the two analyses focused on the basic events associated to the ACC system. In fact, from the analysis presented above a failure of the ACC system is less risk-important when compared to the failure of the LPI or LPR systems.

In order to determine if the acceptance criteria used by the SAPHIRE model were consistent with the ones derived by RELAP5-3D/RAVEN, several reference LBLOCA calculations were performed, changing at each run the actuation time and the availability of the ECCS components. Results from the set of LBLOCA-DEGB calculations are reported in Table 1.

**Table 1. LBLOCA DEGB safety margins results.**

Cases for DEGB LBLOCA		1 <sup>st</sup> PCT (K)	2 <sup>nd</sup> PCT (K)	Margins 1 <sup>st</sup> peak (K)	Margins 2 <sup>nd</sup> peak (K)
Accumulator	LPIS				
0	1	1044.9	1218.8	432.1	258.2
1	1		1002.2		474.8
2	1		913.1		563.9
0	2		1084.5		392.5
1	2		958.1		518.9
2	2		904.6		572.4

The trend of the RPV water level and the PCT for the transients reported in Table 1 are shown in Figure 15. No core damage conditions (PCT>2200 F or 1477 K) were found for the investigated cases.

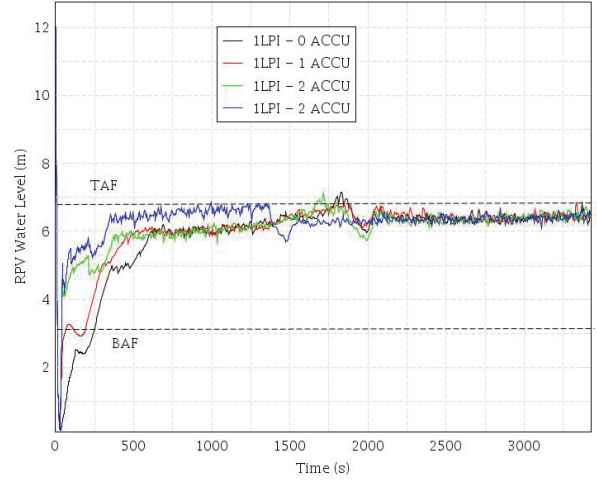
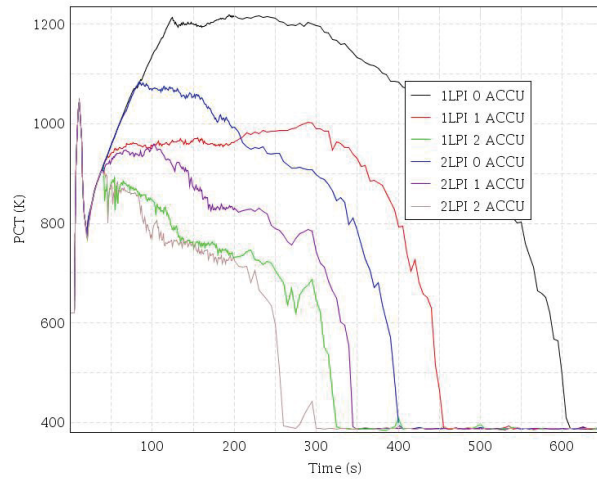


**Figure 15. LBLOCA DEGB cases. PCT (left), RPV level (right).**

## 5. CONCLUSIONS

In this report we have developed a series of risk-informed methods which can be employed to measure risk-importance of system/components using simulation-based PRA methods. The design/development of these methods has been such that they are compatible with risk-importance measures developed for classical PRA methods. A series of analytical tests have been performed in order to prove the validity of such methods using classical reliability models.

We have performed an exhaustive PRA analysis of a PWR system for LLOCA initiating event using RAVEN coupled with RELAP5-3D and compared this analysis with the ones performed by employing classical PRA tools such as SAPHIRE. The comparison of the two sets of results highlighted the limitations of classical PRA methods when employed to analyze complex system such nuclear systems.

The analysis shows how the RISMC approach can be identified as an integrated deterministic and PRA method. Success criteria and timing/sequencing of events are implicitly modeled in the system simulator while stochastic model of systems/components are part of the sampling strategy.

This report can be considered a first step toward addressing the NRC rule 10CFR50.69. The categorization step that is part of the 10CFR50.69 process can in fact be performed by employing the methods presented in this report. Since the analysis performed using the RISMC approach is compatible with classical PRA methods, 10CFR50.69 can be performed by employing both classical and RISMC methods depending on the initiating event.

### 5.1 Publications

During FY17 the following publications were developed:

- Journal papers (see Appendices A and B):
  - D. Mandelli, Z. Ma, C. Parisi, D. Maljovec, A. Alfonsi, C. Smith, “Measuring Risk-Importance in a Simulation-Based PRA Framework - Part I: Mathematical Framework”, Draft for Reliability Engineering and System Safety.
  - D. Mandelli, C. Parisi, Z. Ma, D. Maljovec, A. Alfonsi, C. Smith, “Measuring Risk-Importance in a Simulation-Based PRA Framework - Part II: Comparison Between Simulation-Based and Classical PRA Methods”, Draft for Reliability Engineering and System Safety.
- Conference papers:
  - D. Mandelli, Z. Ma, C. Parisi, A. Alfonsi, C. Smith, “Measuring Risk Importance in a Dynamic PRA Framework,” Proceedings for the Probabilistic Safety Assessment Conference PSA2017, American Nuclear Society (2017).
  - D. Mandelli, A. Alfonsi, C. Smith, “Risk Monitoring Capabilities from Dynamic PRA Data,” Proceedings for the ANS Winter Meeting, American Nuclear Society (2017).

## 6. REFERENCES

- [1] RELAP5-3D Code Development Team, RELAP5-3D Code Manual (2005).
- [2] R. O. Gauntt, "MELCOR Computer Code Manual, Version 1.8.5", Vol. 2, Rev. 2. Sandia National Laboratories, NUREG/CR-6119.
- [3] U.S. Nuclear Regulatory Commission, "Severe accident risks: an assessment for five U.S. nuclear power plants Final Summary Report", NUREG-1150, Washington DC (1990).
- [4] C. Smith, C. Rabiti, And R. Martineau, "Risk Informed Safety Margins Characterization (RISMC) Pathway Technical Program Plan", Idaho National Laboratory technical report: INL/EXT-11-22977 (2011).
- [5] W. Vesely et al., "Measures of risk importance and their applications", NUREC/CR-3385 (1983).
- [6] 10CFR50.69, Risk-Informed Categorization and Treatment of Structures, Systems and Components for Nuclear Power Reactors, Office of the Federal Register, National Archives and Records Administration, U.S. Government Printing Office, Washington, DC.
- [7] E. Zio, M. Marseguerra, J. Devooght, And P. Labeau, "A concept paper on dynamic reliability via Monte Carlo simulation," in *Mathematics and Computers in Simulation*, pp. 47-71 (1998).
- [8] B. Rutt, U. Catalyurek, A. Hakobyan, K. Metzroth, T. Aldemir, R. Denning, S. Dunagan, And D. Kunsman, "Distributed dynamic event tree generation for reliability and risk assessment," in *Challenges of Large Applications in Distributed Environments*, pp. 61-70, IEEE (2006).
- [9] D. Mandelli, Z. Ma, And C. Smith, "Comparison of a traditional probabilistic risk assessment approach with advanced safety analysis," in *Proceeding of American Nuclear Society* (2014).
- [10] D. Mandelli, S. Prescott, C. Smith, A. Alfonsi, C. Rabiti, J. Cogliati, R. Kinoshita, "Modeling of a Flooding Induced Station Blackout for a Pressurized Water Reactor Using the RISMC Toolkit," in *ANS PSA 2015 International Topical Meeting on Probabilistic Safety Assessment and Analysis* Columbia, SC, on CD-ROM, American Nuclear Society, LaGrange Park, IL, 2015.
- [11] R. L. Boring, R. Benish Shirley, J. C. Joe, D. Mandelli, And C. Smith, "Simulation and Non-Simulation Based Human Reliability Analysis Approaches", Idaho National Laboratory technical report: INL/EXT-14-33903 (2014).
- [12] H. S. Abdel-Khalik, Y. Bang, J. M. Hite, C. B. Kennedy, C. Wang, "Reduced Order Modeling For Nonlinear Multi-Component Models," *International Journal on Uncertainty Quantification*, 2 - 4, pp. 341-361 (2012).
- [13] A. Alfonsi, C. Rabiti, D. Mandelli, J. Cogliati, R. Kinoshita, And A. Naviglio, "RAVEN and Dynamic Probabilistic Risk Assessment: Software Overview," in *Proceedings of European Safety and Reliability Conference ESREL* (2014).
- [14] C. Rabiti, A. Alfonsi, J. Cogliati, D. Mandelli, R. Kinoshita, RAVEN, a new software for dynamic risk analysis, in: *Proceedings of the Probabilistic Safety Assessment and Management (PSAM) 12*, 2014.
- [15] D. Mandelli, C. Smith, T. Riley, J. Nielsen, A. Alfonsi, J. Cogliati, C. Rabiti, J. Schroeder, BWR station blackout: A RISMC analysis using RAVEN and RELAP5-3D, *Nuclear Technology* 193 (2016) 161-174.
- [16] K. Fleming, "Developing useful insights and avoiding misleading conclusions from risk importance measures in PSA application", *Proceedings of PSA96, ANS* (1996).
- [17] E. Borgonovo, G. Apostolakis, "A new importance measure for risk-informed decision making", *Reliability Engineering and System Safety*, 72, pp. 193-212 (2011)

- [18] 10CFR50.69 SSC Categorization Guideline, Nuclear Energy Institute, Washington, DC, December 2005, NEI-00-04.

## **APPENDIX A**

D. Mandelli, Z. Ma, C. Parisi, D. Maljovec, A. Alfonsi, C. Smith, “Measuring Risk-Importance in a Simulation-Based PRA Framework - Part I: Mathematical Framework”, Draft for Reliability Engineering and System Safety.

# Measuring Risk-Importance in a Simulation-Based PRA Framework - Part I: Mathematical Framework

D. Mandelli, Z. Ma, C. Parisi, D. Maljovec, A. Alfonsi, C. Smith

*Idaho National Laboratory (INL), 2525 Fremont Ave, 83402 Idaho Falls (ID), USA*

---

## Abstract

Risk importance measures are indexes that are used to rank systems, structures and components (SSCs) using risk-informed methods. The most used/known measures are: Risk Reduction Worth (RRW), Risk Achievement Worth (RAW), Birnbaum (B) and Fussell-Vesely (FV). Once obtained from classical Probabilistic Risk Analysis (PRA) analyses, these risk measures can be effectively employed to relatively rank component importance. In contrast to classical PRA methods, Dynamic PRA methods couple stochastic models with safety analysis codes to determine risk associate to complex systems such as nuclear plants. Compared to classical PRA methods, simulation-based approaches can evaluate with higher resolution the safety impact of timing and sequencing of events on the accident progression. The objective of this paper is to present a series of methods that can be employed to measure risk importance of components which are part of complex systems such as nuclear power plants. The first set of measures are directly derived from classical risk importance measures (e.g., RRW, RAW, B and FV) and that can be employed to any Dynamic PRA analysis. In addition, we provide a set of risk importance measures that capture the dynamic nature of the problem and provide insight related to plant safety margins.

*Keywords:* Importance Measures, Dynamic PRA, Probabilistic Risk Assessment

---

## 1. Introduction

Risk Importance Measures (RIMs) [1] are indexes that are used to rank systems, structures and components (SSCs) based on their contribution to the overall risk. The most used measures [2] are: Risk Reduction Worth (RRW), Risk Achievement Worth (RAW), Birnbaum (B) and Fussell-Vesely (FV).

Typically, this ranking is performed in a classical PRA framework, where risk is determined by considering probability associated to the minimal cut sets generated by static Boolean logic structures [3] (e.g., Event-Trees, Fault-Trees). In a classical PRA analysis, each SSC is represented by a set of basic events; as



10 an example emergency diesel generators can be represented by two basic events:  
failure to start and failure to run.

The risk measures associated to each basic event are calculated from the  
generated cut-sets by determining:

- The nominal risk
- 15 • The increased risk assuming basic event failed
- The reduced risk assuming basic event perfectly reliable

In this context, the Nuclear Regulatory Commission (NRC) has issued the  
10CFR50.69 document [4] allowing plant owners to perform a risk-informed  
categorization and treatment of SSCs in order to reduce operating and mainte-  
20 nance costs while preserving acceptable risk levels. The described categorization  
is based on a set of risk importance measures obtained from the plant classic  
PRA models.

In contrast to classical PRA methods, Dynamic PRA methods [5] couple  
stochastic models (e.g., RAVEN [6], ADAPT [7], ADS [8], MCDET [9]) with  
25 physics-based codes (e.g., RELAP5-3D [10], MELCOR [11], MAAP [12]) to  
determine risk associate to complex systems such as nuclear plants. Accident  
progression is thus determined by the simulation code and not set a-priori by  
the user. The advantage of this approach, compared to classical PRA methods,  
is that a higher realism of the results can be achieved since:

- 30 • No assumption of timing/sequencing of events is assumed by the user  
but,instead, it is dictated by the accident evolution
- No success criteria are defined but, instead, the simulation stops if either  
a fail or a success state are reached
- There is no need to compute convolution integrals in order to specify  
35 probability of basic events that temporally depends on other basic events.
- Addition of scenario-specific information such as timing and complexity  
are available to inform human reliability models.

The scope of this paper is to present a method to determine classical RIMs  
from Dynamic PRA data. Several test cases will be presented in order to show  
40 how the calculation is performed. In addition, new margin-centric RIMs that  
better capture the continuous aspect of a Dynamic PRA approach will be pre-  
sented.

## 2. Classical RIMs

Nuclear industry PRA codes such as SAPHIRE can calculate the following  
45 seven different basic event importance measures for each basic event for the  
respective fault tree, accident sequence, or end state:

- Fussell-Vesely (FV)
- Risk Increase Ratio (RIR)
- Risk Increase Difference (RID)
- 50 • Risk Reduction Ratio (RRR)
- Risk Reduction Difference (RRD)
- Birnbaum (B)
- Uncertainty Importance

The FV importance measure indicates the fraction of the minimal cut set upper bound (or sequence frequency, core damage frequency) contributed by the cut sets containing the basic event of interest. It is calculated in SAPHIRE Version 8 as  $FV = F(i)/F(x)$  where:

- $F(x)$  is the value of all the minimal cut sets evaluated with the basic event probabilities at their mean value
- 60 •  $F(i)$  is the value of all the minimal cut sets that contain the basic event  $i$ .

The RIR or RID importance measure indicates the increase (in relative ratio changes or in actual differences) of the minimal cut set upper bound (or sequence frequency, core damage frequency) when the basic event of interest has failed (i.e., the basic event failure probability is 1.0).

65 The RIR importance is often called Risk Achievement Worth (RAW) in industry. The risk increase importance measures are calculated in SAPHIRE Version 8 as follows:  $RIR = F(1)/F(x)$  and  $RID = F(1) - F(x)$  where:

- $F(x)$  is the value of all the minimal cut sets evaluated with the basic event probabilities at their mean value.
- 70 •  $F(1)$  is the value of all the minimal cut sets evaluated with the probability of the basic event of interest set to 1.0.

The RRR or RRD importance measure indicates the reduction (in relative ratio changes or in actual differences) of the minimal cut set upper bound (or sequence frequency, core damage frequency) if the basic event of interest never fails (i.e., the basic event failure probability is 0.0). The Risk Reduction Ratio importance is also often called RRW in industry. The risk decrease importance measures are calculated in SAPHIRE Version 8 as follows:  $RRR = F(x)/F(0)$  and  $RRD = F(x) - F(0)$  where:

- $F(x)$  is the value of all the minimal cut sets evaluated with the basic event probabilities at their mean values.
- 80 •  $F(0)$  is the value of all the minimal cut sets evaluated with the probability of the basic event of interest set to 0.0.

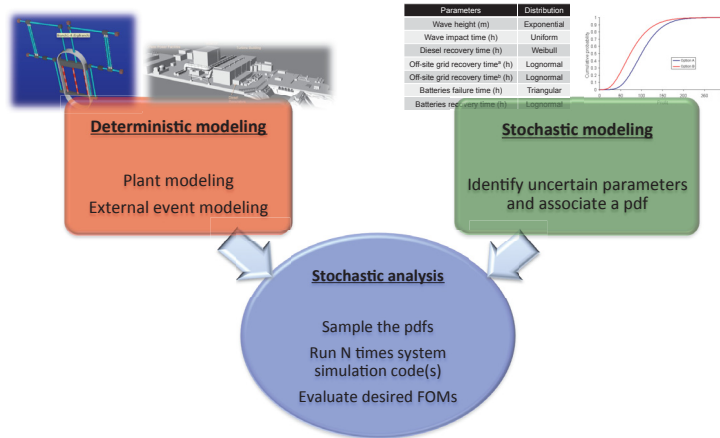


Figure 1: Overview of the RISMC approach

The Birnbaum importance measure is an indication of the sensitivity of the minimal cut set upper bound (or sequence frequency, core damage frequency) with respect to the basic event of interest. It is calculated as  $B = F(1) - F(0)$

- $F(1)$  = value of all the minimal cut sets evaluated with the probability of the basic event of interest set to 1.0.
- $F(0)$  = value of all the minimal cut sets evaluated with the probability of the basic event of interest set to 0.0.

The Uncertainty Importance measure is an indication of the contribution of the basic event of interest uncertainty to the total output uncertainty. This importance measure is not widely used and is not discussed in further detail.

### 3. RISMC Approach to PRA

The Risk Informed Safety MArgin Characterization (RISMC) approach [13] employs both deterministic and stochastic models in a single analysis framework (see Figure 1). In the deterministic method set we include elements such as:

- Modeling of the thermal-hydraulic behavior of the plant [14, 15]
- Modeling of external events such as flooding [16]
- Modeling of the operators responses to the accident scenario [17]

Note that deterministic modeling of the plant or external events can be performed by employing specific simulator codes but also surrogate models [18], known as reduced order models (ROM). ROMs would be employed in order to decrease the high computational costs of high fidelity codes. In addition, multi-fidelity codes can be employed to model the same system; the idea is to switch

105 from low-fidelity to high-fidelity code when higher accuracy is needed (e.g., use low-fidelity codes for steady-state conditions and high-fidelity code for transient conditions)

In the stochastic modeling we include all stochastic parameters that are of interest in the PRA analysis such as uncertain parameters and stochastic failure of system/components. As mentioned earlier, the RISMC approach relies on multi-physics system simulator codes (e.g., RELAP5-3D [10]) coupled with stochastic analysis tools (e.g., RAVEN [19]). From a PRA point of view, this type of simulation can be described by using two sets of variables:

- 115 •  $\mathbf{c} = \mathbf{c}(t)$  represents the status of components and systems of the simulator (e.g., status of pumps and valves)
- $\boldsymbol{\theta} = \boldsymbol{\theta}(t)$  represents the temporal evolution of a simulated accident scenario, i.e.,  $\boldsymbol{\theta}(t)$  represents a single simulation run. Each element of  $\boldsymbol{\theta}$  can be for example the values of temperature or pressure in a specific node of the simulator nodalization.

From a mathematical point of view, a single simulator run can be represented as a single trajectory in the phase space. The evolution of such a trajectory in the phase space can be described mathematically as follows:

$$\begin{cases} \frac{\partial \boldsymbol{\theta}}{\partial t} = \boldsymbol{\Xi}(\boldsymbol{\theta}, \mathbf{c}, \mathbf{s}, t) \\ \frac{\partial \mathbf{c}}{\partial t} = \boldsymbol{\Gamma}(\boldsymbol{\theta}, \mathbf{c}, \mathbf{s}, t) \end{cases} \quad (1)$$

120 where:

- $\boldsymbol{\Xi}$  is the actual simulator code that describes how  $\boldsymbol{\theta}$  evolves in time
- $\boldsymbol{\Gamma}$  is the operator which describes how  $\mathbf{c}$  evolves in time, i.e., the status of components and systems at each time step
- $\mathbf{s}$  is the set of stochastic parameters.

125 Starting from the system located in an initial state,  $\boldsymbol{\theta}(t = 0) = \boldsymbol{\theta}(0)$ , and the set of stochastic parameters (which are generally generated through a stochastic sampling process), the simulator determine at each time step the temporal evolution of  $\boldsymbol{\theta}(t)$ . At the same time, the system control logic determines the status of the system and components  $\mathbf{c}(t)$ .

130 By using the RISMC approach, the PRA analysis is performed by [16]:

1. Associating a probabilistic distribution function (pdf) to the set of parameters  $\mathbf{s}$  (e.g., timing of events)
2. Performing stochastic sampling of the pdfs defined in Step 1
3. Performing a simulation run given  $\mathbf{s}$  sampled in Step 2, i.e., solve the system of equations 1

135

4. Repeating Steps 2 and 3  $M$  times and evaluating user defined stochastic parameters such as core damage (CD) probability ( $P_{CD}$ ).

Note that  $s$  includes not only uncertain parameters characteristic of the simulator (e.g., pipe friction coefficients) but also the set Basic Events (BEs) associated to the considered components.

The goal of measuring components risk importance is to identify the components that contribute the most to the system/plant overall risk.

The objective of this identification process once completed is that plant resources (e.g., procurement costs, maintenance, testing) can be directed towards more risk-significant components or they can be replaced with more reliable models while fewer resources can be allocated to components that are of lower risk.

### 3.1. RISM Approach and Classical PRA

In a classical PRA framework, each BE has a unique probability value associated to it (with possible uncertainty) while in a dynamic PRA each BE has a probability distribution function (pdf) associated to it. This pdf that describes the stochastic behavior of the component can be discrete in nature (e.g., a Bernoulli distribution) or continuous (e.g., exponential).

As an example let's consider two basic events associated to the emergency diesel generators (EDGs) of a nuclear power plant: EDG failure to start ( $EDG_{FS}$ ) and EDG failure to run ( $EDG_{FR}$ ). In a classical PRA framework two probability values would be associated to each basic event:  $p_{EDG_{FS}}$  and  $p_{EDG_{FR}}$ . In a dynamic PRA framework two pdfs would be associated to each basic event:

- $EDG_{FS} \sim \text{Bern}(p_{EDG_{FS}})$  (Bernoulli distribution representing success 0 or failure 1)
- $EDG_{FR} \sim \text{Exp}(\lambda_{EDG_{FR}})$  (Exponential distribution representing the time of failure).

When comparing Dynamic vs. Classical PRA approaches note the following:

- $EDG_{FS}$  has the identical statistical model in the two approaches
- $EDG_{FR}$  has different statistical models; however, if we set

$$p_{EDG_{FR}} = \int_0^{MT} \lambda_{EDG_{FR}} \cdot e^{-\lambda_{EDG_{FR}} t} dt \quad (2)$$

where  $MT$  is the EDG mission time, then the two models are identical from a statistical perspective.

An additional methodological difference among classical and dynamic PRA is the modeling of sequencing and timing of events. In classical PRA this is typically performed using Event-Trees (ETs) where sequence and timing of events are set by the analysis prior to the analysis. An example of an ET is shown in Fig. 2 for large Loss Of Coolant Accident (LOCA): successful outcome of each

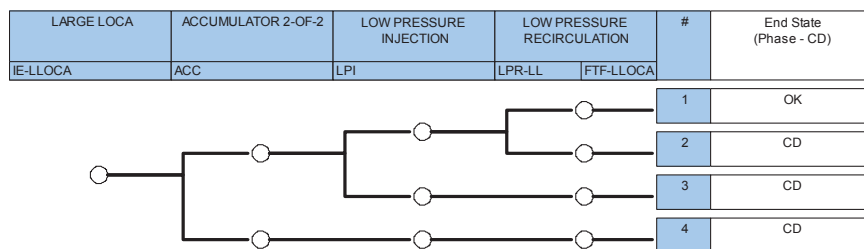


Figure 2: Large LOCA ET.

ET branch is guaranteed only if the accumulator, low-pressure injection (LPI) and low-pressure recirculation (LPR) systems successfully perform their function. Each ET branch corresponds to a possible accident scenario while each branching point corresponds to the successful or failed activation of a system (accumulator, LPI and LPR) The ET construction requires the definition of a set of acceptance criteria (e.g., collapsed level greater than 1/3 of core height) and a set of success criteria for each system involved in the accident progression. This criteria are determined by the analysis and might be backed up by a set of thermal-hydraulic calculations.

In a dynamic PRA method, timing and sequencing of events are uniquely dictated by the system control logic and by the set of stochastic parameters  $\mathbf{s}$ , i.e., the construction of the ET is replaced by coding the plant control logic (e.g., system activation points and activation rules). In addition, acceptance criteria and success criteria are incorporated into the physics model of the code. Back to the large LOCA scenario, in a dynamic framework it would be modeled by:

- Employing a system simulator code (e.g., RELAP5-3D)
- Defining three stochastic parameters:
  - accumulator system: failure on demand (Bernoulli distribution)
  - LPI system: failure to run (Exponential distribution)
  - LPR system: failure to run (Exponential distribution)
- Setting the condition to end a code simulation run and its corresponding outcome:
  - OK outcome: mission time (e.g., 24 hours)
  - Fail outcome: maximum core temperature greater than 2200 F

Note that discrepancies among classical and dynamic PRA methods can occur for sequence of events coupled with system dynamics. Assuming two events A and B occur in sequence and time of activation of each of them is a stochastic variable ( $t_A \sim pdf_A(t)$  and  $t_B \sim pdf_B(t)$ ), the actual activation

time  $T_B$  of system B is a stochastic variable given by the sum of  $t_A$  and  $t_B$  ( $T_B = t_A + t_B$ ). In a classical PRA framework, the distribution of  $T_B$  (i.e.,  $pdf_{A+B}(t)$ ) can be determined by solving the convolution integral:

$$pdf_{A+B}(t) = \int_{-\infty}^{\infty} pdf_B(t - \tau)pdf_A(\tau)d\tau \quad (3)$$

This convolution integral get more complex when accident progression include a large number of events and system dynamics affect timing of events.

#### 4. RAVEN

200 The Risk Analysis and Virtual ENviroment (RAVEN<sup>1</sup>) [6, 19] is a flexible and multi-purpose uncertainty quantification, regression analysis, probabilistic risk assessment, data analysis and model optimization framework. Depending on the tasks to be accomplished and on the probabilistic characterization of the problem, RAVEN perturbs (e.g., Monte-Carlo, latin hypercube, reliability surface search) the response of the system under consideration by altering its own  
 205 parameters. The system is modeled by third party software (e.g., RELAP5-3D [10], MELCOR [11]) and accessible to RAVEN either directly (software coupling) or indirectly (via input/output files). The data generated by the sampling process is analyzed using classical statistical and more advanced data  
 210 mining approaches. RAVEN also manages the parallel dispatching (i.e. both on desktop/workstation and large High Performance Computing machines) of the software representing the physical model. RAVEN heavily relies on artificial intelligence algorithms to construct surrogate models of complex physical systems in order to perform uncertainty quantification, reliability analysis (limit state  
 215 surface) and parametric studies.

By statistical analysis we include:

- Sampling of codes, either stochastic, e.g., Monte-Carlo [20] and Latin Hypercube Sampling (LHS) [21], deterministic (e.g., grid and Dynamic Event Tree (DET) [22, 23]) or adaptive [24, 25]
- 220 • Generation of ROMs [18], also known as Surrogate models
- Post-processing of the sampled data and generation of statistical parameters (e.g., mean, variance, covariance matrix).

Figure 3 shows a general overview of the elements that comprise the RAVEN statistical framework:

- 225 • Model: it represents the pipeline between input and output space. It comprises both codes (e.g., RELAP5-3D [10]) and also ROMs

---

<sup>1</sup>Official website: <https://raven.inl.gov>,  
 GITHUB repository: <https://github.com/idaholab/raven>

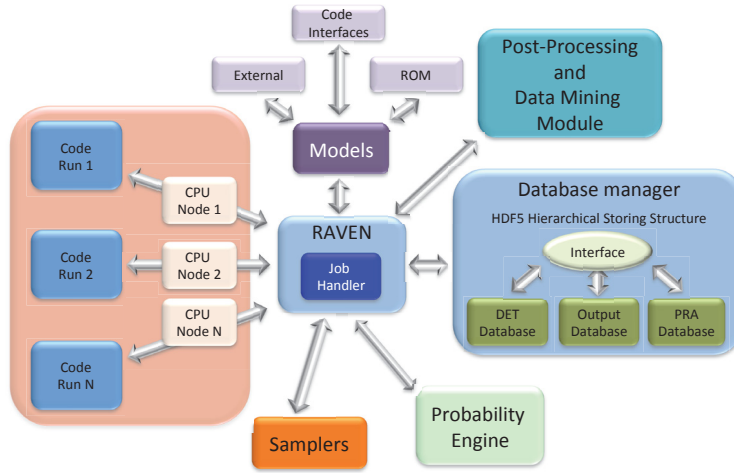


Figure 3: Overview of RAVEN statistical framework components

- Sampler: it is the driver for any specific sampling strategy, e.g., Monte-Carlo, LHS, DET [26, 27])
- Database: the data storing entity
- 230 • Post-processing module: the module that performs statistical analyses and visualizes results.

## 5. Classical RIMs in a Dynamic PRA Context

In a Dynamic PRA environment,  $R_0$  is obtained (e.g., through Monte-Carlo sampling) by:

- 235 1. Running  $N$  simulation (e.g., RELAP5 runs)
2. Counting the number  $N_{CD}$  of simulations that lead to Core Damage (CD) condition
3. Calculating  $R_0 = \frac{N_{CD}}{N}$

Note that while basic events in classical PRA are mainly discrete (binary), in  
 240 a Dynamic PRA environment the sample parameters can be, not only discrete, but more often continuous. As an example, let consider two basic events:

- Emergency Diesel Generator (EDG) failure to start, and,
- EDG failure to run

In classical PRA analyses, a probability value is associated to each basic  
 245 event. In a Dynamic PRA framework, a Bernoulli distribution could be associated to the first basic event and a continuous distribution (e.g., exponential



distribution) could be associated to the second basic event. At this point a challenge arises: the determination of  $R_i^-$  and  $R_i^+$  for each sampled parameter; two possible approaches can be followed :

- 250 1. Perform a Dynamic PRA for  $R_0$  and each  $R_i^-$  and  $R_i^+$  (requiring three times the number of calculations)
2. Determine an approximated value of  $R_i^-$  and  $R_i^+$  from the simulation runs generated to calculate  $R_0$

Regarding Approach 1, given the computational costs of each Dynamic PRA, 255 it is inefficient to determine  $R_i^-$  and  $R_i^+$  for each sampled parameter. In fact, if we consider  $S$  sample parameters (i.e.,  $S$  basic events) over  $N$  simulations, then the risk importance analysis would require  $N(2S + 1)$  simulations.

Regarding Approach 2, a unique method (implemented in RAVEN as an internal post-processor) was developed and it is presented. This method requires 260 input from the user:

- Range,  $I_i^-$ , of the variable  $s_i$  that can be associated to the statement “basic event with component perfectly reliable”
- Range,  $I_i^+$ , of the variable  $s_i$  that can be associated to the statement “basic event in a failed status”

265 Note that the reason we require these types of input in the dynamic analyses is that the parameter space is defined as a continuum unlike the discrete Boolean space found in classical PRA.

Given this kind of information, it is possible to calculate  $R_i^+$  and  $R_i^-$  as follows:

$$R_0 = \frac{N_{CD}}{N} \quad (4)$$

$$R_i^+ = \frac{N_{CD, s_i \in I_i^+}}{N} \quad (5)$$

$$R_i^- = \frac{N_{CD, s_i \in I_i^-}}{N} \quad (6)$$

where:

- 270 •  $N_{CD, s_i \in I_i^+}$  is the number of simulations leading to core damage and with parameter  $s_i \in I_i^+$
- $N_{CD, s_i \in I_i^-}$  is the number of simulations leading to core damage and with parameter  $s_i \in I_i^-$

Since these measures are conditioned on the choices of  $I_i^+$  and  $I_i^-$ , depending on their values,  $R_i^+$  and  $R_i^-$  might change accordingly. In addition, the statistical error associated to the estimates of  $R_i^+$  and  $R_i^-$  also changes as a function of 275 the sampling process. An example is shown in Figure 4 for both cases (discrete and continuous) of a basic event  $x_i$  represented as a stochastic variable which

is sampled (e.g., through a Monte-Carlo process) for each simulation run. If we consider the continuous case and assume  $s_i$  correspond to the basic event “EDG failure to run”. The user might impose the following in order to determine  $R_i^+$  and  $R_i^-$ :

- $I_i^- = [T_i^-, \infty]$  where  $T_i^-$  may be set equal to the simulation mission time (e.g., 24 hours). This implies that a sampled value for EDG failure to run greater than 24 hours implies that the EDG actually does not fail to run (reliability equal to 1.0)
- $I_i^+ = [0, T_i^+]$  where  $T_i^+$  may be set to an arbitrary small value (e.g., 5 min). This implies that a sampled value for EDG failure to run smaller than 5 min implies a reliability almost equal to 0.0

Note that while the definition of  $I_i^-$  is perfectly reasonable, the reader could argue that a smaller interval should be chosen for  $I_i^+$  (e.g., 30 seconds or less). Recall that ideally, a value of  $s_i = 0.0$  should be theoretically chosen (and not an interval); however, given the nature of the distribution this is not usefull. Given the nature of the problem, we are bound to choose an interval  $I_i^+$ :

- A small interval in the region of  $s_i = 0.0$  would lead to a value of  $R_i^+$  close to the theoretical one. However, the number of actual sampled values falling in  $I_i^+$  would be very small, leading to a large stochastic error.
- A large interval in the region of  $s_i = 0.0$  would lead to a value of  $R_i^+$  far from the theoretical one. However, the number of actual sampled values falling in  $I_i^+$  would be very high, i.e., small stochastic error.

A solution to the large statistical error associated to a very small interval  $I_i^+$  can be solved by employing different sampling algorithms other than the classical Monte-Carlo one. As an example, a better resolution of the final value for  $R_i^+$  can be achieved by sampling uniformly the range of variability of  $x_i$  and associate an importance weight to each sample. At this point the counting variable  $N_{CD}$  is weighted by the weight of each sample. By sampling uniformly the range of variability of  $x_i$ , the number of samples in the interval  $I_i^+$  would be significantly higher.

## 6. Test Examples

In order to better understand the results obtained in this section, it is worth to illustrate a link between classical PRA and RISMC approach. Let’s consider a system that is composed by two components (i.e, A and B) in a series configuration where each component has a failure probability (i.e.,  $p_A$  and  $p_B$  respectively) as shown in Fig. 5.

In a classical PRA framework such system can be modeled using a FT method that is composed by two basic events: A failed and B failed. System failure would be represented by a single “AND” gate that combine the two basic events as shown in Fig. 5.

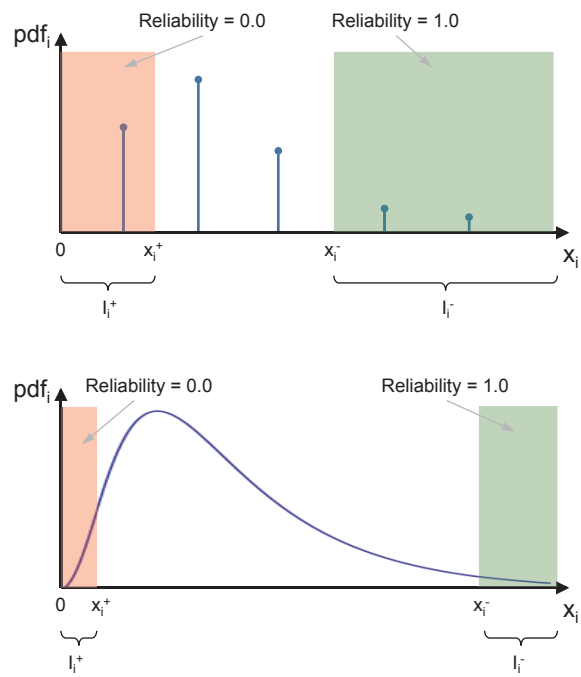


Figure 4: Treatment of discrete (top) and continuous (bottom) stochastic variables for reliability purposes.

In a RISMCM approach, such system would be modeled by using two stochastic parameters (i.e.,  $var_A$  and  $var_B$ ) with a Bernoulli distribution  $Bern(p)$  associated to each of them:  $var_A \sim Bern(p_A)$  and  $var_B \sim Bern(p_B)$ . The model that emulates system response would simply implement the “AND” logic of the  $var_A$  and  $var_B$ . In order to determine system failure probability a numerical integration has to be performed in a 2-dimensional (a dimension for each stochastic parameter).

Two possible sampling strategies can be followed:

- Monte-Carlo: generate  $N$  samples and count the the number of samples that lead to system failure
- Grid: partition the 2-dimensional space into a Cartesian grid; generate a sample for each partition and associate a probability weight  $w$  to each sample. This weight can be determined by integrating the pdf  $pdf(A, B) = Bern(p_A)Bern(p_B)$  in each partition. In this specific case, since each stochastic parameter has two possible outcomes (i.e. 0 and 1), the space has been partitioned into 4 regions as shown in Fig. 6. Each cell of Fig. 6 has indicated the system outcome: system failure (F) or system success (OK).

The Monte-Carlo approach would require a large number of samples in order to decrease the statistical error associated to system failure probability. On the other hand, a Grid sampler would determine the exact value of system failure probability with only 4 samples:

1. sample 1:  $A = 0$  and  $B = 0$  (bottom left cell of Fig. 6),  $w_1 = (1 - p_A) \cdot (1 - p_B)$
2. sample 2:  $A = 1$  and  $B = 0$  (top left cell of Fig. 6),  $w_2 = p_A(1 - p_B)$
3. sample 3:  $A = 0$  and  $B = 1$  (bottom right cell of Fig. 6),  $w_3 = (1 - p_A) \cdot p_B$
4. sample 4:  $A = 1$  and  $B = 1$  (top right cell of Fig. 6),  $w_4 = p_A \cdot p_B$

Note that each sample/cell of Fig. 6 that leads to system failure corresponds to a specific cut-set

- Cut-set 1 (CS1) corresponds to sample 2;  $p_{CS1} = p_A$
- Cut-set 2 (CS2) corresponds to sample 3;  $p_{CS2} = p_B$
- Cut-set 3 (CS3) corresponds to sample 4;  $p_{CS3} = p_A \cdot p_B$

Hence, the two methods (classical and PRA) would provide identical results.

Observe now that the number of samples required for  $M$  stochastic parameters (assuming they are all distributed with a Bernoulli distribution) would be equal to  $2^M$ . Thus this strategy can be employed for a small value of  $M$ .

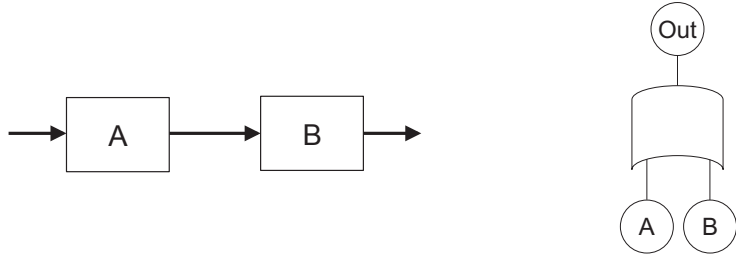


Figure 5: Components A and B in a series configuration (left) and its associated Fault-Tree (right).

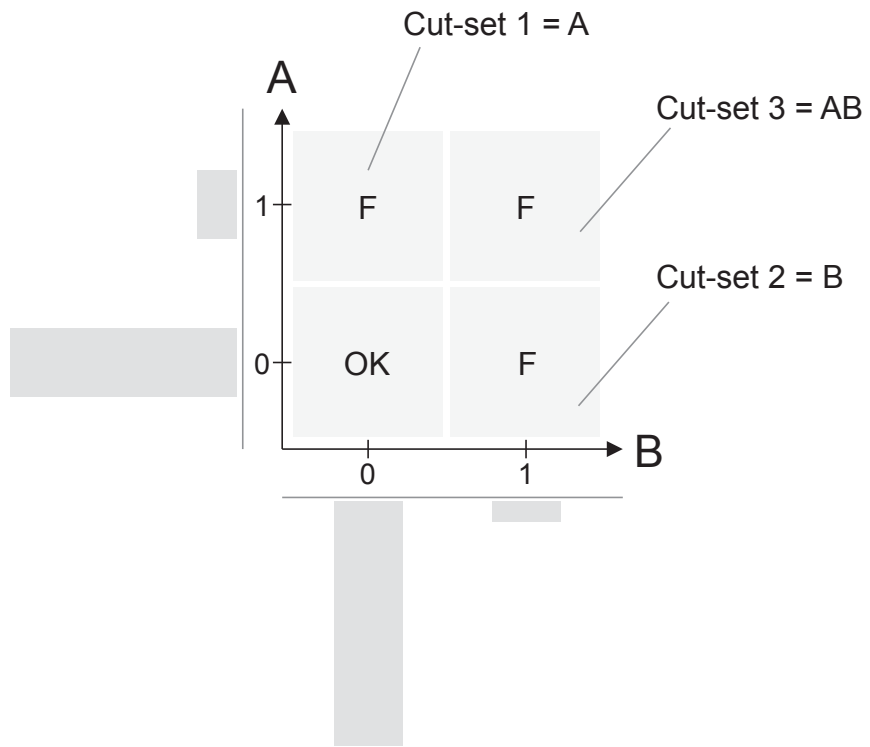


Figure 6

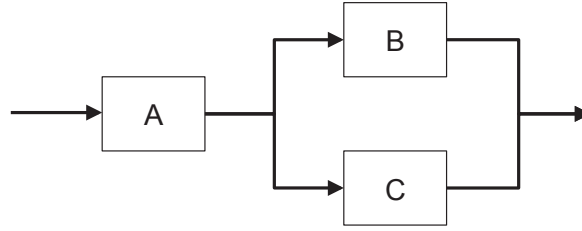


Figure 7: System considered for Examples 1 and 2.

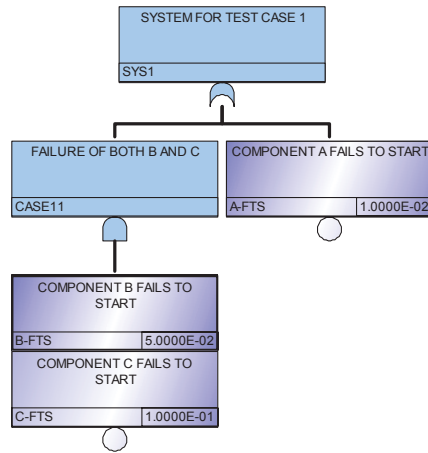


Figure 8: FT structure for the system shown in Fig. 7.

### 6.1. Example 1: series/parallel configuration

355 The first example consists of 3 components arranged in a series/parallel configuration as shown in Fig. 7. In this case the following probabilities of failures (on-demand) are provided:

- $p_A = 1.0 \cdot 10^{-2}$
- $p_B = 5.0 \cdot 10^{-2}$
- 360 •  $p_C = 1.0 \cdot 10^{-1}$

From a classical PRA perspective, this system can be modeled using a FT as shown in Fig. 8.

From a RISM (i.e., dynamic PRA) point of view the analysis of this system is performed as follows (see Section 3.1):

- 365 • Define 3 stochastic parameters (i.e.,  $S = 3$ ):
  - $s_1$ : status of component A
  - $s_2$ : status of component B

Table 1: Results obtained for Example 1.

	Analytical	SAPHIRE	RAVEN
$FV_A$	0.67	0.67	0.67
$FV_B$	0.33	0.34	0.33
$FV_C$	0.33	0.34	0.33

	Analytical	SAPHIRE	RAVEN
$RAW_A$	66.9	66.9	66.9
$RAW_B$	7.3	7.3	7.3
$RAW_C$	3.98	3.98	3.98

–  $s_3$ : status of component C

- Assign a distribution to each stochastic parameter; in this case a Bernoulli distribution
- Define  $I_i^+$  and  $I_i^-$  for each distribution: in this case we have chosen  $I_i^- = [0.0, 0.1]$  and  $I_i^+ = [1.0, 1.1]$
- Generate  $N$  samples, for example by employing Monte-Carlo or Grid sampling strategies
- Determine  $R_0$ ,  $R_i^-$  and  $R_i^+$  for each component
- Determine the desired RIMs for each component

Note that a Monte-Carlo sampling is not the best sampling strategy in terms of computational costs. This is even more relevant if the value of  $p_A$ ,  $p_B$  or  $p_C$  were several order of magnitude lower.

A more effective sampling strategy would be the Grid sampling (see Section 3.1): the stochastic variables are sampled over a fixed Cartesian grid and a probability weight is associated to each sample. In this case, each stochastic variable  $s_i$  is sampled over two values, 0.0 and 1.0, and the probability weights  $w_i^0$  and  $w_i^1$  values associated to each sample coordinate are:

- $s_i = 0.0$ :  $w_i^0 = \text{prob}(s_i \in [-\infty, 0.5])$
- $s_i = 1.0$ :  $w_i^1 = \text{prob}(s_i \in [0.5, +\infty])$

Following this grid sampling strategy, only  $2^3 = 8$  are needed. Table 1, the FV and RAW importance values for all three components obtained by RAVEN (using a Grid sampling strategy) are shown compared with the analytical ones.

## 6.2. Example 2: time-dependent stand-by configuration

The second example considers a simplified ECCS model (see Fig. ??) of a reactor. It consists of the following components and for a subset of them a value of mean time to failure (MTTF) is provided:

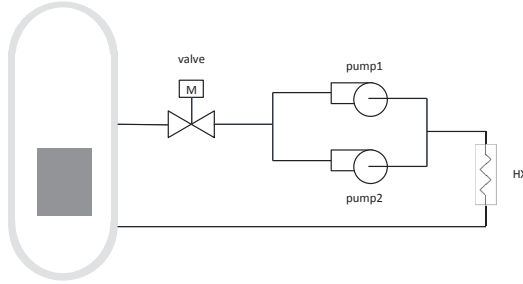


Figure 9: System considered for Example 3.

Table 2: Results obtained for Example 2.

	Analytical	SAPHIRE	RAVEN
$FV_{valve}$	0.30	0.69	0.30
$FV_{pump1}$	0.26	0.82	0.26
$FV_{pump2}$	0.26	0.82	0.26

	Analytical	SAPHIRE	RAVEN
$RAW_{valve}$	1.18	1.10	1.18
$RAW_{pump1}$	1.12	1.05	1.12
$RAW_{pump2}$	1.12	1.05	1.12

- Motor-operate valve M (MTTF = 24 h,  $\lambda_{valve} = 0.041667$ )
- 395 • Two redundant pumps, pump1 and pump2 (MTTF = 12 h,  $\lambda_{pump1} = \lambda_{pump2} = 0.083333$ )
- Heat exchanger HX (reliability = 1.0)

Pump1 is normally used while pump2 is on standby. If Pump1 fails then pump2 provide water flow in a switching arrangement. Pump2 cannot fail while  
 400 in standby. Switch from pump1 to pump2 is perfectly reliable. The cooling is such that it takes 2 hours to reach vessel failure condition if the M-pump1-pump2 system has failed. Mission time is again equal to 24 hours.

Note in this case classical PRA methods require model adjustments via convolution calculations in order to correctly determine system reliability. Table 2  
 405 are shown the FV importance for all three components obtained by RAVEN (using a Monte-Carlo sampling strategy) compared with the analytical ones.

### 6.3. Example 3: $K$ out of $N$ configuration

The third example is similar to the one shown in Section 6.2 It consists of the following components:

- 410 • Motor-operate valve M (MTTF = 24 h,  $\lambda_{valve} = 0.041667$ )



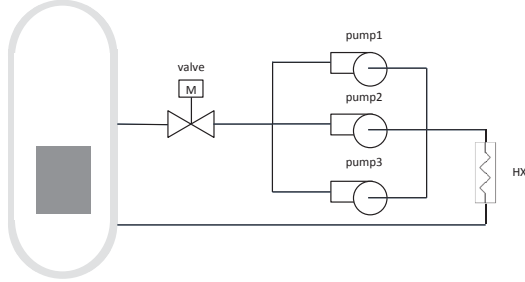


Figure 10: System considered for Example 3.

Table 3: Results obtained for Example III.

	Analytical	SAPHIRE	RAVEN
$FV_{valve}$	0.032	0.64	0.033
$FV_{pump1}$	0.076	0.94	0.081
$FV_{pump2}$	0.076	0.94	0.081
$FV_{pump3}$	0.076	0.94	0.081

	Analytical	SAPHIRE	RAVEN
$RAW_{valve}$	1.02	1.0	1.02
$RAW_{pump1}$	1.01	1.0	1.01
$RAW_{pump2}$	1.01	1.0	1.01
$RAW_{pump3}$	1.01	1.0	1.01

- Three pumps, pump1, pump2 and pump3 (MTTF = 12 h,  $\lambda_{pump1} = \lambda_{pump2} = \lambda_{pump3} = 0.083333$ )
- Heat exchanger HX (reliability = 1.0)

All pumps are initially running but 2 out of 3 are required to cool the system.  
 415 Mission time is again equal to 24 hours.

Table 3 are shown the FV importance for all three components obtained by RAVEN (using a Monte-Carlo sampling strategy) compared with the analytical ones.

#### 6.4. Example 4: time and physics dependent stand-by configuration

420 The fourth example considers the system of Example 2 (see Section 6.2) but it considers also the temporal behavior of the reactor. The top event is not the failure of valve-pump1-pump2 system but it occurs when core temperature  $T$  reaches a threshold value  $T_{max}$  (i.e., reactor failure). Mission time is still 24 hours.

425 Note that the configuration is slightly different from the one presented in the first two examples (here a stand-by configuration is introduced) but also the condition of system failure is dictated by the dynamic behavior of the PWR.

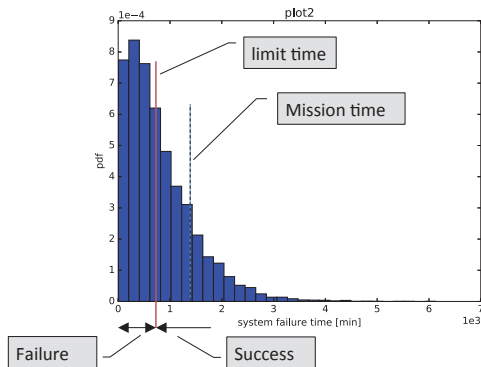


Figure 11

Table 4: Results obtained for Example 4.

	FV	RAW
valve	0.58	2.21
pump1	0.28	1.48
pump2	0.28	1.48

The system is designed such that a late failure of the ECCS may not lead to system failure (i.e., natural circulation is providing enough cooling). In other words, the ECCS is vital especially in the hours right after a reactor scram.

In principle, this test case cannot be solved analytically due to the complexity of the reactor behavior. It can be solved by identifying the time  $T_{lim}$  (limit time) after which a failure of the valve-pump1-pump2 system does not cause reactor failure since natural circulation can provide enough cooling. Note that  $T_{lim}$  could only be determined by recursively running the system simulator until a good estimate of  $T_{lim}$  is reached.

Figure 11 shows the histogram of the failure time of valve-pump1-pump2 system along with the limit time  $T_{lim}$  for the two different power levels (100% and 120%). Note that a higher power level implies a faster reactor heatup rate; hence, the valve-pump1-pump2 system must provide more cooling before the natural circulation can sustain a failure of the valve-pump1-pump2 system:  $T_{lim}$  increases.

#### 6.4.1. Considerations on the mission time

In the example presented in Section 6.4 two code stopping conditions were: core temperature greater than 2200 F and simulation time reaches 24 hours (mission time). Note that the mission time stopping condition imposes that a simulation is considered successful even if the valve-pump1-pump2 system has failed and the reactor temperature increases; if a longer mission time would be chosen then the simulation would be classified no longer with an OK outcome but with a fail outcome. Thus, special attention has been given to the assumptions

behind the mission time.

Depending on the employed code simulator the best solution is to re-define the mission time  $T_{miss}$  as the time below which events can occur; in addition, the code is set to end the simulation not when the mission time is reached but at a time  $T_{end} = T_{miss} + T_{relax}$  where the addition of  $T_{relax}$  allows the simulation to reach a steady-state condition.

#### 6.4.2. Considerations on the sampling strategy

In order to get accurate results of the risk importance measures the number of simulation runs to perform can be very high (order of thousands and up). In addition, given that each simulation run may require hours of simulation time, this kind of analysis may be feasible only for large high performance computing systems.

An alternative approach is to employ ROMs instead of the actual simulation code so that a large number of data points can be generated in a much faster time on standard computing machines. In this case the approach would be as follows:

1. Generate a limited set of sample points using the simulation code
2. Train and validate a ROM given the data set generated in Step 1
3. Perform the analysis with the ROM obtained in Step 2

The training and creation of the ROM can be performed in several ways; for the applications targeted by this paper we have found two optimal choices.

The first one explores the totality of input space uniformly and it reconstructs the response of the code in the input space.

The second one exploits the binary nature of the problem (i.e., the outcome of each simulation run is binary: either OK or failed) and it try to determine the limit surface: the boundaries in the input space that separate failure region (i.e., characterized by the undesired simulation outcome; e.g., core damage) from success region (i.e., characterized by the desired simulation outcome; e.g., max clad temperature below 2200 F). This sampling strategy, called “adaptive sampling” (or smart sampling), can obtain much better statistical results since the the code response is queried in the most relevant zones of the input space (the limit surface).

The steps for the adaptive sampling strategy are:

1. Perform a set of runs of the simulator code: the number of required runs may depend on the dimensionality of the input space
2. Given the set of simulation runs obtained in Step 1, create a ROM. The objective of this ROM is to infer the response of the simulator code, i.e., create an approximate output given the same set of input parameters
3. Identify a set of points on the limit surface
4. Chose a subset of points from the ones obtained in Step 4
5. Perform a simulation run for each of the points obtained in Step 5 using the simulator code
6. Repeat Steps 2 through 6 until convergence is reached

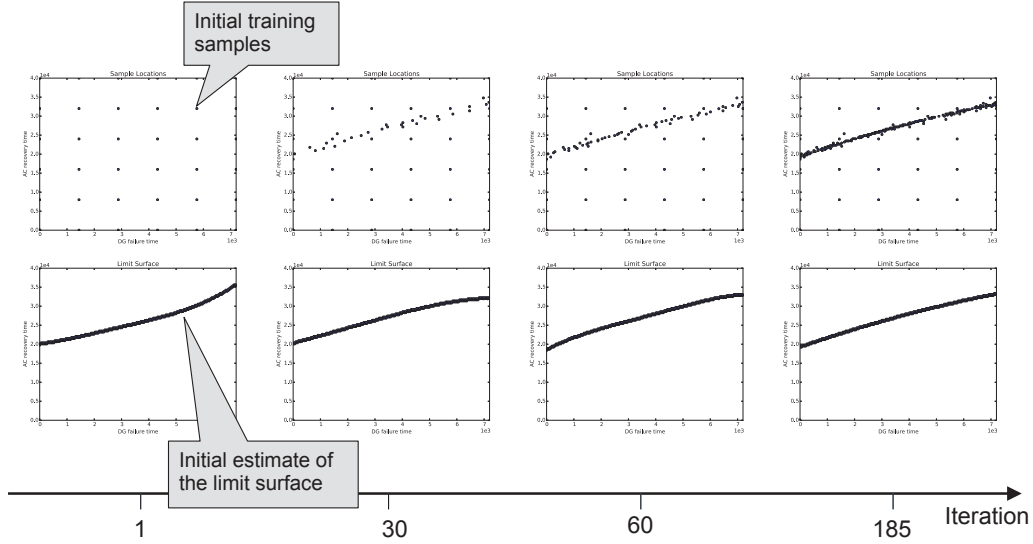


Figure 12: Example of adaptive sampling

An example of adaptive sampling is shown in Fig. 12 for a 2-dimensional case. Figure 12 shows the location of the chosen sample points and the estimate of the limit surface as the iteration illustrated above progresses. Note that the code is evaluated in a safety strategic area: the limit surface.

## 7. Extension To Time-Dependent Data

In order to extend the calculation presented in Section 5 in the time-domain we need additional information: the temporal profile of the status of those components that might be taken offline due to maintenance or testing.

We will follow this notation:

- $\Xi$  represents the system configuration, i.e., the status of components and systems of the plant on the time scale  $\tau$  of the plant lifetime
- $RAW_i(\tau)$ ,  $FV_i(\tau)$ ,  $RRW_i(\tau)$ ,  $B_i(\tau)$  are the RIMs determined for the basic event  $i$  calculated on the time scale  $\tau$

Note that in our application the status of each component can be only binary: component operating or component off-line (i.e., either because it is failed or under maintenance/testing). Thus component performance degradation is not considered. The calculation algorithms is as follows given a set of simulated data:

1. Divide the temporal profile into  $L$  segments where the status of the components, i.e. the system configuration  $\Xi$ , remain constant
2. For each time segment, i.e., for  $l = 1, \dots, L$

2.1. Determine  $R_0$  according to the system configuration  $\Xi_l$  for segment  $l$

$$R_0(l) = \frac{N_{CD, \Xi = \Xi_l}}{N_{\Xi = \Xi_l}} \quad (7)$$

515 2.2. For each component determine  $R_i^-$  and  $R_i^+$

- If the component is on-line,  $R_i^-$  and  $R_i^+$  are determined as follows:

$$R_i^+(l) = \frac{N_{CD, s_i \in I_i^+, \Xi = \Xi_l}}{N_{\Xi = \Xi_l}} \quad (8)$$

$$R_i^-(l) = \frac{N_{CD, s_i \in I_i^-, \Xi = \Xi_l}}{N_{\Xi = \Xi_l}} \quad (9)$$

- If the component is off-line determine  $R_i^+(l)$  according to Eq. ?? and set  $R_i^-(l) = R_i^+(l)$

### 7.1. Test case

520 For the scope of this paper we have chosen an example that can help the reader to understand the proposed algorithm. This a simple system composed of three components (i.e., A, B and C) in a parallel/series configuration shown in Figure 7. To each component a failure rate is provided when the system is called on demand:

- $\lambda_A = 1.0 \cdot 10^{-3} hr^{-1}$
- 525 •  $\lambda_B = 5.0 \cdot 10^{-3} hr^{-1}$
- $\lambda_C = 1.0 \cdot 10^{-2} hr^{-1}$

530 Even though the system can be solved analytically we have chosen a dynamic method to solve it in order to show how the proposed methods is implemented. By using a Monte-Carlo based Dynamic PRA method, we have generated a database of simulated data where each data point is structured as follows:

- Input variables: failure time of components A, B and C (i.e.,  $s_i$ ) sampled from their own distribution (i.e., exponential with lambda values provided at the beginning of this section)
- Output variables: status of the system (either OK or CD)

535 We have selected the temporal profile for two components: A and C as shown in Fig. 13. By following the algorithm presented above it has been possible to determine the temporal profiles of:

- system failure probability (see Fig. 14 left)
- RIMs such as FV (see Fig. 14 right)

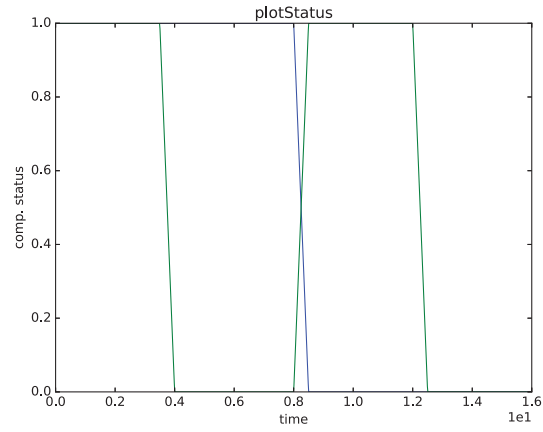


Figure 13: Temporal profile of the status for component A (blue line) and C (green line).

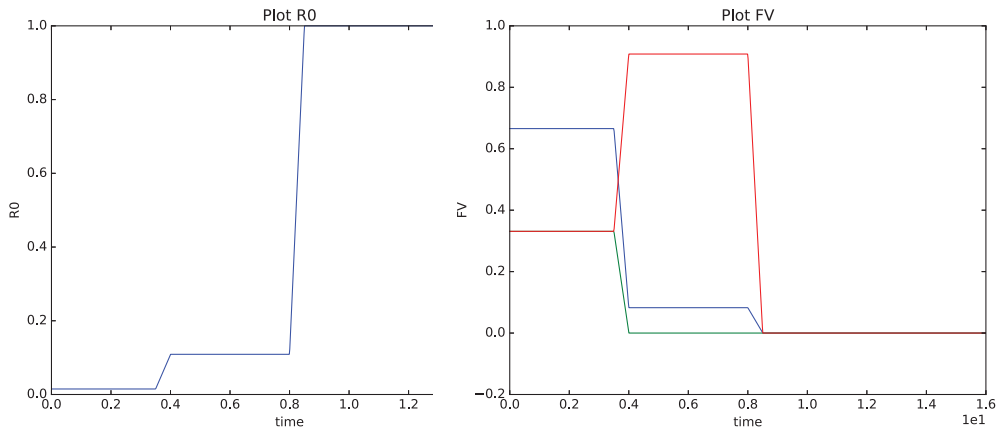


Figure 14: Temporal profile for system failure probability (left) and FV profile (right) for components B (green line), A (blue line) and C (red line).

540 **8. New RIMs in a Dynamic PRA Context**

Note that the RIMs described so far are tied to a binary logic of the outcome variable (e.g., OK vs. CD). Dynamic PRA approaches typically generate a continuous value of the outcome variables (e.g., peak clad temperature -  $PCT$ ). In our application (see previous sections) we typically convert  $PCT$  to a discrete one as follows:

- $PCT > 2200F$ : outcome = CD
- $PCT < 2200F$ : outcome = OK

550 Given the different structure of the approach used in this paper to solve a PRA problem (i.e., Dynamic instead of classical PRA), the reader might think that a different set of RIMs should/could be developed in order to capture the nature of the problem solved using Dynamic PRA. As a starting point, it would be worth investigating the nominal probabilistic distribution (pdf) of  $PCT$  with the one obtained when reliability of each basic event (sampled parameter) is 0.0 or 1.0. So now we can indicate:

- 555
- $pdf_0(T)$ : nominal pdf of  $PCT$
  - $pdf_i^-(T)$ : pdf of  $PCT$  associated to basic event  $i$  assuming basic event is perfectly reliable
  - $pdf_i^+(T)$ : pdf of  $PCT$  associated to basic event  $i$  assuming basic event has failed

An example is shown below for a hypothetical case where the obtained  $pdf_0(T)$  is indicated using a histogram while the limit value for  $PCT$  is shown using the red line passing at 2200 F. In order to make a connection to what has been presented in the previous section, note that by looking at Fig. 15:

$$R_0 = \int_{2200}^{\infty} pdf_0(T) dT \quad (10)$$

As part of the RISM analysis, the user might want to supplement the results obtained in the previous section with the information associated to a more effective margin analysis. In particular, of interest for RISM applications is (see Fig. 15) the concept of margin:

$$margin = 2200 - PCT \text{ given } PCT < 2200 \quad (11)$$

560 Using the same philosophy indicated in the previous section for classical RIMs, we want to determine:

- $margin_0$ : pdf of the variable  $2200 - PCT$  given that  $PCT < 2200$
- $margin_i^-$ : pdf of the variable  $2200 - PCT$  given that  $PCT < 2200$  for basic event  $i$  assuming it is perfectly reliable

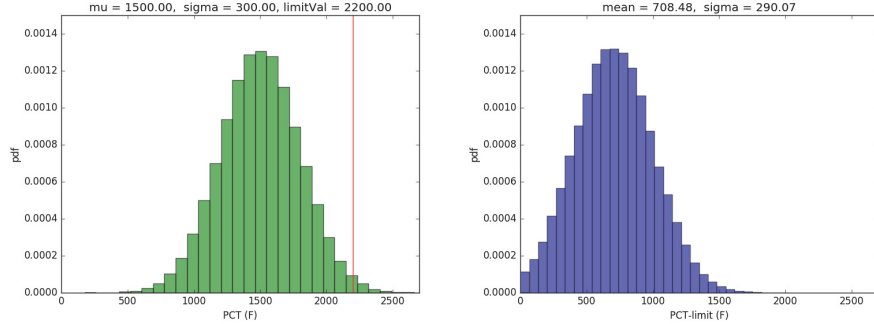


Figure 15: Plot of a hypothetical  $pdf_0(T)$  (left) and its associated margin  $margin_0$  (right).

- 565
- $margin_i^+$ : pdf of the variable  $2200 - PCT$  given that  $PCT < 2200$  for basic event  $i$  when its assumed to be failed

Note now that  $margin_0$ ,  $margin_i^-$  and  $margin_i^+$  are pdfs and not numerical values. Hence, now the challenge arises on how to compare two pdfs:

- $margin_0$  vs.  $margin_i^-$
- 570 •  $margin_0$  vs.  $margin_i^+$

Assume two pdfs are given:  $pdf_1(x)$  and  $pdf_2(x)$ . A couple of approaches can be followed: Z-test or KolmogorovSmirnov test. In the first approach (Z-test), the following variable  $Z$  is computed:

$$Z_{1,2} = \frac{mean(pdf_1) - mean(pdf_2)}{\sqrt{std\_dev^2(pdf_1) - std\_dev^2(pdf_2)}} \quad (12)$$

where:

- $mean(pdf)$  correspond to the mean of  $pdf(x)$
- $std\_dev(pdf)$  correspond to the standard deviation of  $pdf(x)$

In the second approach (KolmogorovSmirnov test), instead of the pdf, the cumulative distribution functions (pdf) are considered:  $cdf_1(x)$  and  $cdf_2(x)$ . In particular, the Kolmogorov-Smirnov statistic is calculated as:

$$Z_{1,2} = \sup_x (cdf_1(x) - cdf_2(x)) \quad (13)$$

- 575 Note that so far we have imposed clad failure temperature ( $CFT$ ) to be a fixed value, i.e., 2200 F. In many RISMC applications  $CFT$  is no longer a numerical value but it can be an uncertain parameter, i.e., a pdf is associated to CDF:  $pdf(T)$ . This tie goes back to the original logo of RISMC where a pdf



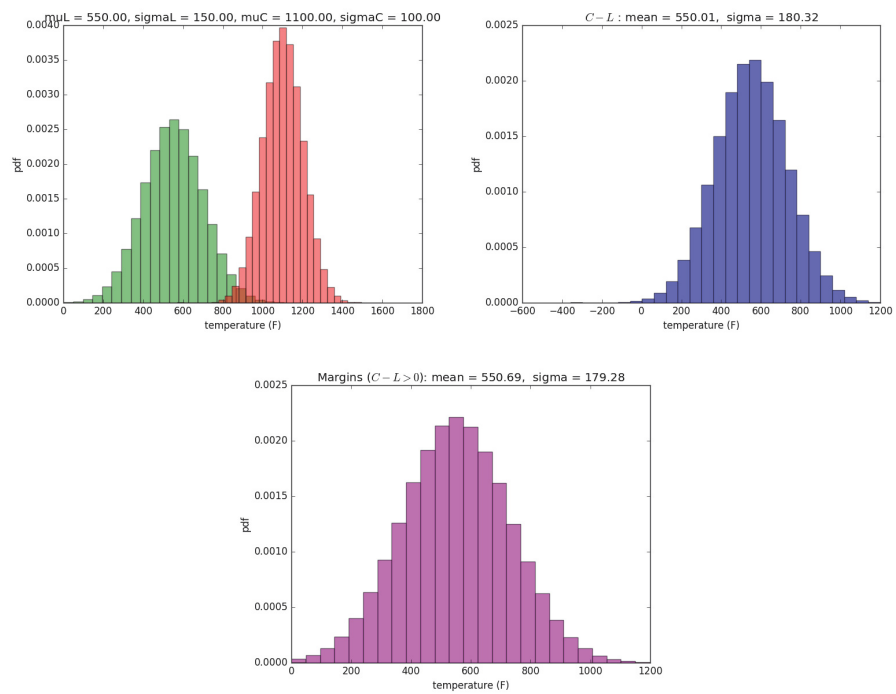


Figure 16: Plot of the pdfs for  $PCT$  (green) and  $CFT$  (red) (top left), Plot of the pdf of the variable  $CFT - PCT$  (top right) and Plot of the pdf of the margin, i.e.,  $CFT - PCT > 0$  (bottom).

for “load” and “capacity” (see Fig. 16). A new definition of margin can be then defined:

$$margin = (CFT - PCT) \text{ given } (CFT - PCT > 0) \quad (14)$$

580 Once the pdf associated to the margin variable is determined it is possible to employ either the Z-tests or the KolmogorovSmirnov test in order to measure how this pdf changes when each basic event is considered perfectly reliable or failed.

## 9. Conclusions

585 This paper has presented a mathematical framework for determining risk importance measures in a simulation based, i.e. dynamic, PRA framework. We have shown how classical measures can be derived and we have provided few explanatory examples. We have also indicated how the data generation method is important to maximize the amount of information generated by each simulation run. Lastly we have presented a novel set of risk importance measures 590 that are not bounded by a Boolean logic but explore the continuity of the problem. The advantage of these measures is that they capture the idea of “safety margin”.

## Appendix A: Analytical Results

595 *Example 1*

For the system described in Section 6.1 we have the following

$$R_0 = p_A + p_B p_C - p_A p_B p_C = 0.01495 \quad (15)$$

$$R_A^- = p_B p_C = 0.005 \quad (16)$$

$$R_A^+ = 1.0 \quad (17)$$

$$R_B^- = p_A = 0.01 \quad (18)$$

$$R_B^+ = p_A + p_C - p_A p_C = 0.109 \quad (19)$$

$$R_C^- = p_A = 0.01 \quad (20)$$

$$R_C^+ = p_A + p_B - p_A p_B = 0.0595 \quad (21)$$

Thus:

$$FV_A = \frac{R_0 - R_A^-}{R_0} = 0.665552 \quad (22)$$

$$FV_B = \frac{R_0 - R_B^-}{R_0} = 0.331104 \quad (23)$$

$$FV_C = \frac{R_0 - R_C^-}{R_0} = 0.331104 \quad (24)$$

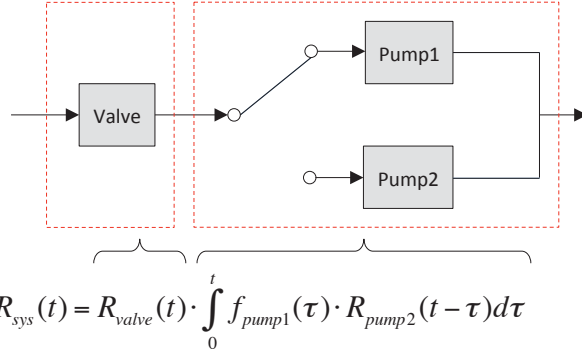


Figure 17: Reliability block diagrams for Example 2 (see Section 6.2).

and:

$$RAW_A = \frac{R_i^+}{R_0} = 66.88963 \quad (25)$$

$$RAW_B = \frac{R_i^+}{R_0} = 7.29097 \quad (26)$$

$$RAW_C = \frac{R_i^+}{R_0} = 3.97993 \quad (27)$$

*Example 2*

We can solve the system described in Section 6.2 using reliability block diagrams (see Fig. 17).

Thus time dependent reliability of the system  $R_{sys}(t)$  as function of time  $t$ :

$$R_{sys}(t) = R_{valve}(t) \int_0^t f_{pump1}(\tau) R_{pump2}(t - \tau) d\tau \quad (28)$$

600 where:

- $R_{valve}(t) = e^{-\lambda_{valve}t}$
- $f_{pump1}(t) = \lambda_{pump1}e^{-\lambda_1t}$
- $R_{pump2}(t) = e^{-\lambda_{pump2}t}$

It can be shown that if  $\lambda_{pump1} = \lambda_{pump2} = \bar{\lambda}$ :

$$R_{sys}(t) = e^{-\lambda_{valve}t} [e^{-\bar{\lambda}}(1 + \bar{\lambda}t)] \quad (29)$$

For this system we have the following for a mission time  $T = 24$  hours:

$$R_0 = 1.0 - R_{sys}(T) = 0.85063876 \quad (30)$$

$$R_{valve}^- = 1.0 - [e^{-\bar{\lambda}T}(1 + \bar{\lambda}T)] = 0.593994129 \quad (31)$$

$$R_{valve}^+ = 1.0 \quad (32)$$

$$R_{pump1}^- = 1.0 - R_{valve}(T) = 0.6321205 \quad (33)$$

$$R_{pump1}^+ = 1.0 - R_{valve}(T)R_{pump2}(T) = 0.95021292 \quad (34)$$

$$R_{pump2}^- = R_{pump1}^- = 0.6321205 \quad (35)$$

$$R_{pump2}^+ = R_{pump1}^+ = 0.95021292 \quad (36)$$

### Example 3

We can solve the system described in Section 6.2 using again reliability block diagrams. Thus time dependent reliability of the system  $R_{sys}(t)$  as function of time  $t$ :

$$R_{sys}(t) = R_{valve}(t)R_{2oo3}(t) \quad (37)$$

605 where  $R_{2oo3}(t)$  represents reliability of a set of three identical components in a 2 out of 3 (2oo3) configuration.

It can be shown that if  $\lambda_{pump1} = \lambda_{pump2} = \lambda_{pump3} = \bar{\lambda}$  (thus  $R_{pump1}(t) = R_{pump2}(t) = R_{pump3}(t) = \bar{R}(t) = e^{-\bar{\lambda}t}$ ) then  $R_{2oo3}(t)$  can be written as

$$R_{2oo3}(t) = \sum_{n=2}^3 \binom{3}{n} \bar{R}(t)^n [1 - \bar{R}(t)]^{3-n} = 3e^{-2\bar{\lambda}t}(1 - e^{-\bar{\lambda}t}) + e^{-3\bar{\lambda}t} \quad (38)$$

For this system we have the following for a mission time  $T = 24$  hours:

$$R_0 = 1.0 - R_{sys}(T) = 0.981609917 \quad (39)$$

$$R_{valve}^- = 1.0 - R_{2oo3}(T) = 0.95001058 \quad (40)$$

$$R_{valve}^+ = 1.0 \quad (41)$$

$$R_{pump1}^- = 1.0 - R_{1oo2}(T)R_{valve}(T) = 0.907163789 \quad (42)$$

$$R_{pump1}^+ = 1.0 - R_{valve}(T)\bar{R}(t)^2 = 0.993262051 \quad (43)$$

$$R_{pump2}^- = R_{pump1}^- \quad (44)$$

$$R_{pump2}^+ = R_{pump1}^+ \quad (45)$$

$$R_{pump3}^- = R_{pump1}^- \quad (46)$$

$$R_{pump3}^+ = R_{pump1}^+ \quad (47)$$

where  $R_{1oo2}(t)$  represents reliability of a set of two identical components in a 1 out of 2 (1oo2) configuration:

$$R_{1oo2}(t) = \sum_{n=1}^2 \binom{2}{n} \bar{R}(t)^n [1 - \bar{R}(t)]^{2-n} = 2e^{-\bar{\lambda}t}(1 - e^{-\bar{\lambda}t}) + e^{-2\bar{\lambda}t} \quad (48)$$

## References

- 610 [1] W. E. Vesely, T. C. Davis, R. S. Denning, N. Saltos, NUREC/CR-3385: Measures of Risk Importance and their Applications, Technical Report, U.S. Nuclear Regulatory Commission, Washington DC, 2005.
- [2] K. Fleming, Developing useful insights and avoiding misleading conclusions from risk importance measures in PSA application, in: Proceedings of PSA 1996 International Topical Meeting On Probabilistic Safety Assessment And Analysis, 1996.
- 615 [3] U. S. NRC, NUREC/CR-1150: Severe Accident Risks: An Assessment For Five U.S. Nuclear Power Plants Final Summary Report, Technical Report, U.S. Nuclear Regulatory Commission, Washington DC, 2005.
- [4] U. S. NRC, 10CFR50.69, Risk-Informed Categorization and Treatment of Structures, Systems and Components for Nuclear Power Reactors, Technical Report, U.S. Nuclear Regulatory Commission, Washington DC, 2004.
- [5] J. Devooght, C. Smidts, Probabilistic dynamics as a tool for dynamic PSA, *Reliability Engineering & System Safety* 52 (1996) 185 – 196.
- 625 [6] C. Rabiti, A. Alfonsi, J. Cogliati, D. Mandelli, R. Kinoshita, RAVEN, a new software for dynamic risk analysis, in: Proceedings of the Probabilistic Safety Assessment andnd Management (PSAM) 12, 2014.
- [7] B. Rutt, U. Catalyurek, A. Hakobyan, K. Metzroth, T. Aldemir, R. Denning, S. Dunagan, D. Kunsman, Distributed dynamic event tree generation for reliability and risk assessment, in: 2006 IEEE Challenges of Large Applications in Distributed Environments, 2006, pp. 61–70.
- 630 [8] K. S. Hsueh, A. Mosleh, The development and application of the accident dynamic simulator for dynamic probabilistic risk assessment of nuclear power plants, *Reliability Engineering & System Safety* 52 (1996) 297–314.
- [9] E. Hofer, M. Kloos, B. Krzykacz-Hausmann, J. Peschke, M. Woltereck, An approximate epistemic uncertainty analysis approach in the presence of epistemic and aleatory uncertainties, *Reliability Engineering & System Safety* 77 (2002) 229–238.
- 635 [10] R. C. D. Team, RELAP5-3D Code Manual, Technical Report, Idaho National Laboratory Technical Report, 2005.
- [11] R. O. Gauntt, MELCOR Computer Code Manual, Version 1.8.5, Vol. 2, Rev. 2, Sandia National Laboratories, NUREG/CR-6119, 2000.
- [12] EPRI, Modular Accident Analysis Program 5 (MAAP5) Applications Guidance: Desktop Reference for Using MAAP5 Software - Phase 2 Report, Technical Report, Electric Power Reserach Institute, Palo Alto (CA), 2013.
- 645

- [13] C. Smith, C. Rabiti, R. Martineau, Risk Informed Safety Margins Characterization (RISMC) Pathway Technical Program Plan, Technical Report, Idaho National Laboratory Technical Report: INL/EXT-11-22977, 2011.
- 650 [14] D. Mandelli, C. Smith, T. Riley, J. Nielsen, A. Alfonsi, J. Cogliati, C. Rabiti, J. Schroeder, BWR station blackout: A RISMC analysis using RAVEN and RELAP5-3D, Nuclear Technology 193 (2016) 161–174.
- [15] D. Maljovec, S. Liu, B. Wang, D. Mandelli, P. T. Bremer, V. Pascucci, C. Smith, Analyzing simulation-based PRA data through traditional and topological clustering: A BWR station blackout case study, Reliability Engineering & System Safety 145 (2015) 262–276.
- 655 [16] D. Mandelli, S. Prescott, C. Smith, A. Alfonsi, C. Rabiti, J. Cogliati, R. Kinoshita, Modeling of a flooding induced station blackout for a pressurized water reactor using the RISMC toolkit, in: Proceedings of PSA 2015 International Topical Meeting On Probabilistic Safety Assessment And Analysis, 2015.
- 660 [17] R. L. Boring, R. B. Shirley, J. C. Joe, D. Mandelli, C. Smith, Simulation And Non-Simulation Based Human Reliability Analysis Approaches, Technical Report, Idaho National Laboratory Technical Report: INL/EXT-14-33903, 2014.
- 665 [18] H. S. Abdel-Khalik, Y. Bang, J. M. Hite, C. B. Kennedy, C. Wang, Reduced order modeling for nonlinear multi-component models, International Journal On Uncertainty Quantification (2012) 341–36.
- [19] A. Alfonsi, C. Rabiti, D. Mandelli, J. Cogliati, R. Kinoshita, A. Naviglio, RAVEN and dynamic probabilistic risk assessment: Software overview, in: Proceedings of European Safety and Reliability Conference (ESREL 2014), Wroklaw (Poland), 2014.
- 670 [20] E. Zio, M. Marseguerra, J. Devooght, P. Labeau, A concept paper on dynamic reliability via monte carlo simulation, Mathematics And Computers In Simulation 47 (1998) 371–382.
- 675 [21] J. C. Helton, F. J. Davis, Latin hypercube sampling and the propagation of uncertainty in analyses of complex systems, Reliability Engineering & System Safety 81 (2003).
- [22] A. Amendola, G. Reina, DYLAM-1, a software package for event sequence and consequence spectrum methodology, in: EUR-924, CEC-JRC. ISPRA: Commission of the European Communities, 1984.
- 680 [23] G. Cojazzi, The DYLAM approach for the dynamic reliability analysis of systems, Reliability Engineering and System Safety 52 (1996) 279–296.

- 685 [24] C. Rabiti, D. Mandelli, A. Alfonsi, J. Cogliati, R. Kinoshita, Introduction of supervised learning capabilities of the RAVEN code for limit surface analysis, in: Proceedings of American Nuclear Society (ANS), Reno (NV), 2014.
- [25] D. Mandelli, C. Smith, Adaptive sampling using support vector machines, in: Proceeding of American Nuclear Society (ANS), San Diego (CA), volume 107, 2012, pp. 736–738.
- 690 [26] A. Alfonsi, C. Rabiti, D. Mandelli, J. Cogliati, R. Kinoshita, Adaptive dynamic event tree in RAVEN code, in: Proceedings of American Nuclear Society (ANS), Anaheim (CA), 2014.
- 695 [27] A. Alfonsi, C. Rabiti, D. Mandelli, J. Cogliati, R. Kinoshita, A. Naviglio, Dynamic event tree analysis through RAVEN, in: Proceedings of PSA 2013 International Topical Meeting on Probabilistic Safety Assessment and Analysis Columbia, SC, on CD-ROM, American Nuclear Society, LaGrange Park, IL, 2013.

## **APPENDIX B**

D. Mandelli, C. Parisi, Z. Ma, D. Maljovec, A. Alfonsi, C. Smith, “Measuring Risk-Importance in a Simulation-Based PRA Framework - Part II: Comparison Between Simulation-Based and Classical PRA Methods”, Draft for Reliability Engineering and System Safety.



# Measuring Risk-Importance in a Simulation-Based PRA Framework - Part II: Comparison with Classical PRA Methods

D. Mandelli, C. Parisi, Z. Ma, D. Maljovec, C. Smith

*Idaho National Laboratory (INL), 2525 Fremont Ave, 83402 Idaho Falls (ID), USA*

---

## Abstract

In the past decade several advanced Dynamic Probabilistic Risk Analysis (PRA) methods have been developed. These methods couple stochastic methods (e.g., RAVEN, ADAPT, ADS, MCDDET) with safety analysis codes (e.g., RELAP5-3D, MELCOR, MAAP) to determine risk associated to complex systems such as nuclear plants. Compared to classical PRA methods, which are based on static Boolean logic structures (e.g., Event-Trees -ET-, Fault-Trees -FT-), they can determine risk associated to complex systems with higher resolution since they implicitly model timing and sequencing of events on the accident progression. In the first part of this article we have presented a set of risk importance measures that can be employed on a dataset generated by any Dynamic PRA method to rank components based on their importance from a safety point of view. Such measures have been developed as a natural extension of ones employed in industry PRA codes and they have been tested on several analytical test cases. In this second part of the article we show a full comparison between classical and Dynamic PRA methods. The system considered for the comparison is a Pressurized Water Reactor (PWR) system for a large break Loss Of Coolant Accident (LOCA) initiating event. We show how the Dynamic and the ET/FT models have been built from both a stochastic and accident progression point of view. Metrics of comparison are based not only on the core damage probability but also based on the importance values associated to each basic event.

*Keywords:* Importance Measures, Dynamic PRA, Probabilistic Risk Assessment

---

## 1. Introduction

In the past decades, several numerical simulation codes have been employed to simulate accident dynamics, e.g., RELAP5-3D [1], MELCOR [2] or MAAP [3]. In order to evaluate the impact of uncertainties into accident dynamics, several stochastic methodologies have been coupled with these codes. These stochastic methods range from classical Monte-Carlo and Latin Hypercube sampling to stochastic polynomial methods. Similar approaches have been introduced

into the risk and safety community where stochastic methods, e.g., RAVEN [4], ADAPT [5], MCDET [6] or ADS [7], have been coupled with safety analysis codes in order to evaluate the safety impact of timing and sequencing of events on the accident progression. These approaches are usually called Dynamic PRA methods [8].

Compared to classical PRA methods, which are based on static Boolean logic structures (e.g., Event-Trees -ET-, Fault-Trees -FT-), they can determine risk associated to complex systems with higher resolution since the implicitly model timing and sequencing of events on the accident progression. In ET/FT based methods accident progression is fixed and it is set prior the analysis by the analyst. Such approximation is even more limiting for accident scenarios in which tight timing dependencies of events are coupled with plant dynamics (e.g., recovery actions and human related actions).

The scope of this paper is to present a comparison between Dynamic and classical PRA methods. The system considered is a Pressurized Water Reactor (PWR) for a large break Loss Of Coolant Accident (LOCA), LB-LOCA, initiating event.

The comparison Dynamic and classical PRA methods is based not only on the core damage probability but also based on the importance values associated to each basic event.

In [9] we have presented a set of risk importance measures that can be employed on a dataset generated by any Dynamic PRA method to rank components based on their importance from a safety point of view. Such measures have been developed as a natural extension of the ones employed in industry PRA codes such SAPHIRE [10] or CAFTA [11].

In this paper we employs such metrics extensively in order to quantify such comparison. The objectives are twofold: the first one is to validate the proposed metrics over an industry-grade test case and show capabilities of Dynamic PRA methods. The second one is to provide guidance on how it is possible to have classical and dynamic PRA methods compatible with each other. The rationale behind it is that a Dynamic PRA analysis can be performed for a limited aspect of the overall system and its result incorporated into a classical PRA results. Similarly, a classical PRA analysis can be “made dynamic” by adding dynamic elements (e.g., quantitative information of timing of events) into it and coupled with a system simulation code.

## 2. Test Case

The test case considered in this paper is a 3-loop PWR system of Westinghouse design with a large-dry containment. The initiating event is a LB-LOCA: a double-ended guillotine break of one the three hot legs.

Under these accident conditions, the system experiences a sudden sub-cooled blowdown and primary system pressure drops from about 2200 psi down to the saturation pressure (about 1000 psi).

50 In order to compensate the large loss of coolant inventory into the vessel and prevent core damage, two emergency core-cooling systems are employed: Accumulators and Low-Pressure Injection System (LPIS).

Accumulators are passive components consisting of pressurized water tanks that are employed at the beginning of the transient and can dump large inventory of sub-cooled water into the vessel.

55 The LPIS is activated when primary system pressure falls below 980 psi and by using pumps large amount of water are transferred from the Reactor Water Storage Tank (RWST) directly into the vessel.

60 The large amount of water that leaves the primary system and is collected in the containment and, thus, its temperature and pressure increases. In order to cool it down, Containment Sprays (CSs) are employed. Similarly to the LPIS, through pumps RWST water is sprayed from the top level of the containment.

Once RWST is empty, both CSs and LPISs switch from injection mode to recirculation mode: water collected at the base of the containment and through the sump and is injected back into the vessel (through the LPI) and into the containment (through the CSs).

### 3. Comparison Workflow

The comparison between Classical (using SAPHIRE) and Dynamic PRA analysis (using RAVEN/RELAP5-3D) has been performed following these steps:

- 70 1. Simplify the SAPHIRE FT structure by grouping its basic events into macro basic events
2. Perform calculation of the ET-FT model: determine CD probability, probability of each ET branch and the risk importance of each macro basic events
- 75 3. Consider the SAPHIRE ET for the LLOCA initiating event and model the RELAP5-3D accident progression following consistently with the ET logic.
4. Construct the PWR logic based on the same macro basic events determined in Step 1: these macro basic events constitute the stochastic variables sampled by RAVEN
- 80 5. Perform a dynamic analysis using RAVEN/RELAP5-3D for the system constructed in Steps 4 and 5, and determine probability of each ET branch and the risk importance of each macro basic events
6. Compare the results obtained in Steps 3 and 5

85 Step 1 has been deemed necessary in order to limit the number of unnecessary RELAP5-3D simulation runs. The rationale is that each basic event in the set of FTs are also stochastic variables sampled by RAVEN. If all basic events are considered (about a hundred) then the sampling strategy would require a very large number of RELAP5-3D simulation runs. The great majority of these runs would be identical since the impact of these basic events on accident progression is the same.

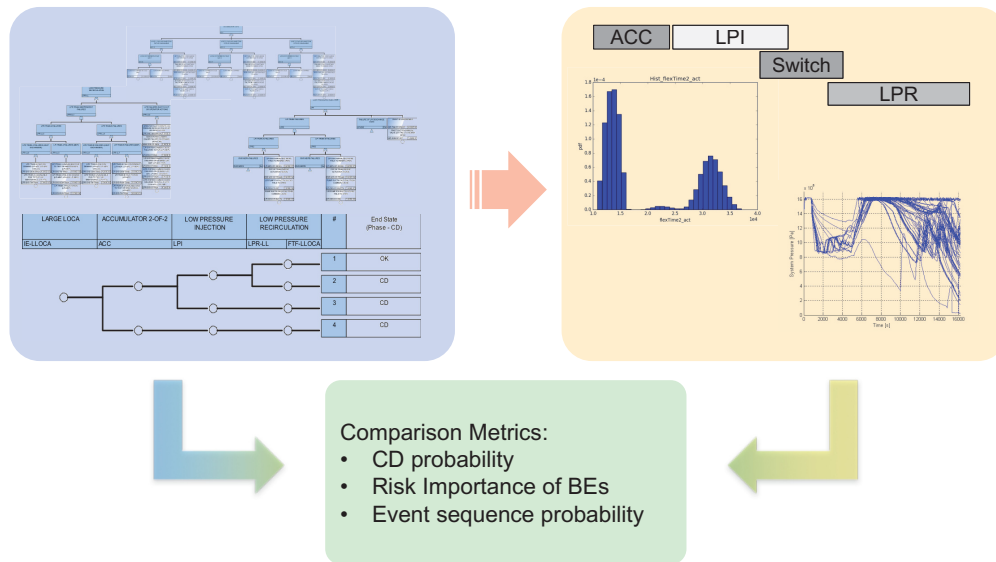


Figure 1: Comparison overview.

The main target of this comparison is to identify commonalities and inconsistencies between Classical and Dynamic PRA methods on the accident progression level (i.e., at the ET level) while the FT level is modeled in the same way for both methods.

#### 4. SAPHIRE Modeling

This section provides an overview of the risk importance measures in SAPHIRE PRA code [10], the introduction of the classical LB-LOCA PRA model for a generic 3-loop pressurized water reactor (PWR), the process to simplify the typical LB-LOCA PRA model as needed, and the importance measure results from the reformulated PRA model that could be compared with those from the corresponding RAVEN/RELAP5 simulation model.

##### 4.1. Risk Importance Measures in SAPHIRE

The SAPHIRE code can calculate the following different basic event importance measures for each basic event of the respective fault tree, accident sequence, or end state:

- Fussell-Vesely (FV)
- Risk Increase Ratio (RIR)
- Risk Increase Difference (RID)

110

- Risk Reduction Ratio (RRR)
- Risk Reduction Difference (RRD)
- Birnbaum (B)
- Uncertainty Importance

The most used importance measures are Fussell-Vesely, Risk Increase Ratio, Risk Reduction Ratio, and Birnbaum. The Fussell-Vesely importance measure indicates the fraction of the minimal cut set upper bound (or sequence frequency, core damage frequency) contributed by the cut sets containing the interested basic event. It is calculated with the following equation:

$$FV = F(i)/F(x) \quad (1)$$

where:

115

- $F(x)$  is the value of all the minimal cut sets evaluated with the basic event probabilities at their mean value.
- $F(i)$  is the value of all the minimal cut sets that contain the interested basic event  $i$ .

The Risk Increase Ratio, which is often called Risk Achievement Worth (RAW), or Risk Increase Difference importance measure indicates the increase (in relative ratio changes or in actual differences) of the minimal cut set upper bound (or sequence frequency, core damage frequency) if the interested basic event always occurred (i.e., the basic event failure probability is 1.0). The risk increase importance measures are calculated with the following equations:

$$RAW = F(1)/F(x) \quad RID = F(1) - F(x) \quad (2)$$

120 where  $F(1)$  is the value of all the minimal cut sets evaluated with the interested basic event probability set to 1.0.

The Risk Reduction Ratio, which is often called Risk Reduction Worth (RRW), or Risk Reduction Difference importance measure indicates the reduction (in relative ratio changes or in actual differences) of the minimal cut set upper bound (or sequence frequency, core damage frequency) if the interested basic event never occurred (i.e., the basic event failure probability is 0.0). The risk reduction importance measures are calculated with the following equations:

$$RRW = F(x)/F(0) \quad RRD = F(x) - F(0) \quad (3)$$

where  $F(0)$  is the value of all the minimal cut sets evaluated with the interested basic event probability set to 0.0. The Birnbaum importance measure is an indication of the sensitivity of the minimal cut set upper bound (or sequence frequency, core damage frequency) with respect to the interested basic event. It is calculated by the following equation:

$$B = F(1) - F(0) \quad (4)$$

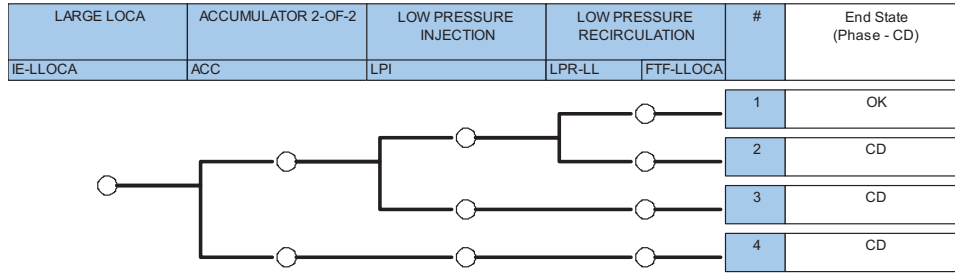


Figure 2: LB-LOCA ET

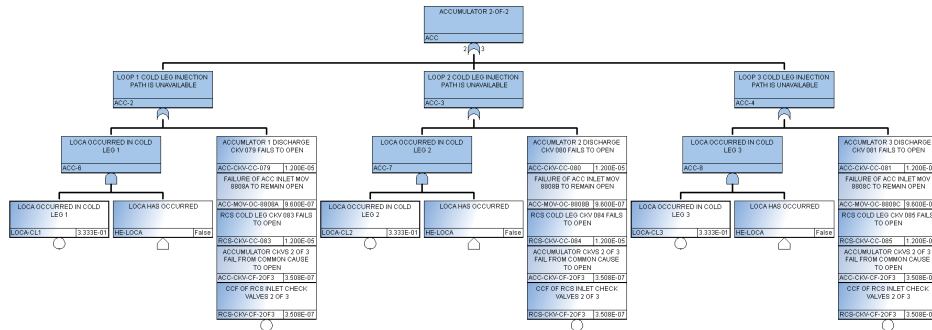


Figure 3: ACC FT

The Uncertainty Importance measure is an indication of the contribution of the interested basic events uncertainty to the total output uncertainty. This importance measure is not used in this paper and not discussed in further detail.

#### 4.2. SAPHIRE LB-LOCA Model

125 Figure 2 shows a typical LB-LOCA event tree that one would find in a classical PRA model. The LB-LOCA event tree has three top events: ACC for accumulator injection, LPI for low pressure safety injection, and LPR-LL for low pressure safety injection during recirculation phase. Each top event is modeled in one or more fault trees. Figure 3 and Figure 4 show the fault trees for ACC and LPI. The LB-LOCA model is quantified with a cutoff value of 1E-12. Its core damage frequency (CDF) is 2.04E-8/year. There are 180 minimum cut sets. Of more than two hundreds basic events in the LB-LOCA model, 60 basic events appear in the 180 minimum cut sets and thus have importance measures. The reported importance measures include Fussell-Vesely, RAW, RRW, and Birnbaum. 41 out of the 60 basic events can be regarded as risk significant using the ASME/ANS PRA Standard definition, i.e.,  $FV \geq 5E-3$  or  $RAW \geq 2$ .

To analyze the LB-LOCA model under the RAVEN/RELAP5 environment,

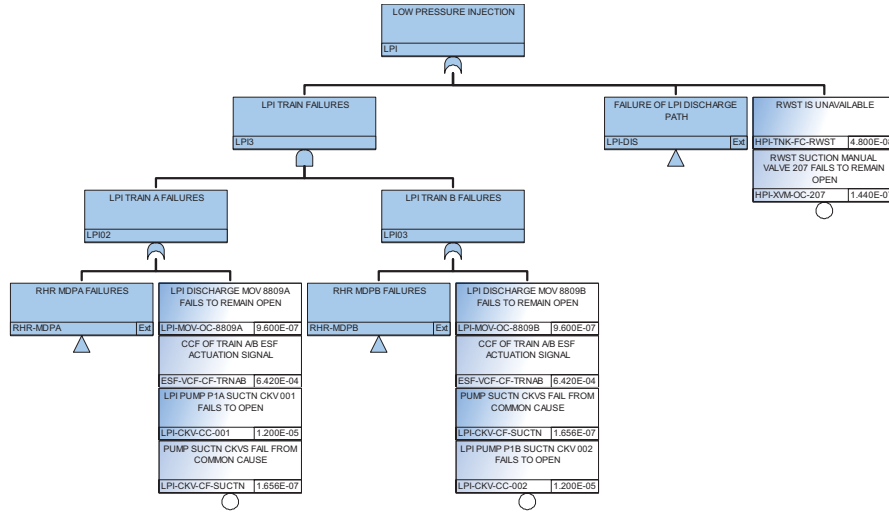


Figure 4: LPI FT

the number of basic events to be simulated is expected to be reduced to less than 20 in order for successful simulation runs. To compare the results from classical PRA with those from simulations, the traditional LB-LOCA model above has to be simplified significantly (with less than 20 unique basic events) while keep the PRA model fidelity as much as possible. The following three-stage progressive process is used in this paper to simplify a traditional PRA model:

- Stage 1, simplify the traditional PRA model by keeping only the cut set basic events (the basic events appear at least once in the minimum cut sets) in the model. All other basic events and subtrees that do not include any such cut set basic events are removed from the model. The simplified Stage 1 model should have the same quantification results (CDF, minimum cut sets, and importance measures) as the original model.
- Stage 2, further simplify Stage 1 model by keeping only the risk significant basic events ( $FV \geq 5E - 3$  or  $RAW \geq 2$ ) in the model. Other non-significant basic events are removed from the model. Stage 2 model would produce different quantification results (CDF, minimum cut sets, and importance measures), however, the differences should not be large.
- Stage 3, simplify Stage 2 model by combining the risk significant basic events to reduce the total basic event number to the expected level. In general, the original basic events could be combined into the following super basic events:
  - System/train or inter-system level failure on demand super basic events, which may include pump fails to start, valve fails to open, etc.

- System/train or inter-system level failure to run super basic events, which may include pump fails to run, heat exchanger fails to transfer heat, containment sump failures, etc.
- System/train or inter-system level unavailable due to test or maintenance super basic events
- Operator action failure super basic events
- Common cause failure on demand super basic event
- Common cause failure to run super basic event

This would create new basic events that group and replace the original basic events and different quantification results with different cut set basic events. The new basic events are used as inputs to the RAVEN/RELAP5 simulation model, and the SAPHIRE results can be compared directly with those from the simulation model. The process is applied to the traditional LB-LOCA model as described in the following sections. Due to the relative simplicity of the LB-LOCA model, Stage 2 of the above process (i.e., removing non risk significant basic events from the model) is deemed not necessary. The 60 LB-LOCA cut set basic events are combined into super basic events directly, and the process is reduced from 3 stages to 2 stages.

#### 4.2.1. Simplifying LB-LOCA PRA Model Stage 1

In Stage 1 of the simplifying LB-LOCA PRA model process, all basic events not reside in any of the minimum cut sets/importance measure results are removed from the fault tree logic. All subtrees are also deleted if they include no cut set basic events. Figure 5 shows an example of such process, in which LPI fault tree is simplified to include only the cut set basic event ESF-VCF-CF-TRNAB and sub-trees RHR-MDPA and RHR-MDPB. All other basic events (LPI-CKV-CC-001, LPI-CKV-CC-002, LPI-CKV-CF-SUCTN, LPI-MOV-OC-8809A, and LPI-MOV-OC-8809B) are removed from the logic. Subtree LPI-DIS is also removed from the logic. Note that LPI-DIS actually includes cut set basic events, RCS-CKV-CC-083, RCS-CKV-CC-084, and RCS-CKV-CC-085, however, these basic events appear in the cut sets from the ACC logic instead of LPI/LPI-DIS logic. As such, the basic events and the subtree could be removed with no impact on the quantification results. Other subtrees that are removed from the logic include AC and DC related subtrees such as ACP-1AA02, DCP-PNL1AD11 under the LPR-LL main fault tree.

#### 4.2.2. Simplifying LB-LOCA PRA Model Stage 2

In Stage 2 (or Stage 3 in a three-stage process) of the simplifying LB-LOCA PRA model process, the 60 cut set basic events retained in Stage 1 model are combined into the following super basic events:

- System/train or inter-system level failure on demand super basic events, which may include pump fails to start, valve fails to open, etc.



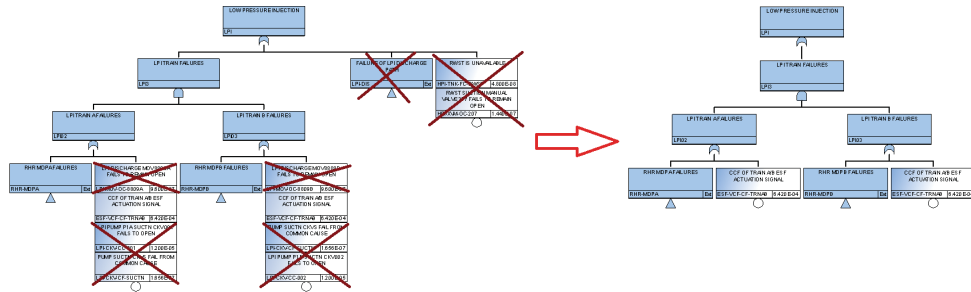


Figure 5: stage1

- System/train or inter-system level failure to run super basic events, which may include pump fails to run, heat exchanger fails to transfer heat, containment sump failures, etc.
- System/train or inter-system level unavailable due to test or maintenance super basic events
- Operator action failure super basic events
- Common cause failure on demand super basic event
- Common cause failure to run super basic event

In ACC fault tree, ACC-CKV-CC-079 and RCS-CKV-CC-083 are grouped into ACC-CKV-CC-CL1 for Accumulator 1 failure to inject. ACC-CKV-CC-080 and RCS-CKV-CC-084 are grouped into ACC-CKV-CC-CL2 for Accumulator 2 failure. ACC-CKV-CC-081 and RCS-CKV-CC-084 are grouped into ACC-CKV-CC-CL3 for Accumulator 3 failure. Figure 6 presents the simplified Stage 2 ACC fault tree. In LPI fault tree (including its subtrees), low pressure injection motor-driven pump A fails to start (LPI-MDP-FS-1A), operator fails to restore LPI MDP A after test maintenance (LPI-XHE-XR-P1A), and LPI Train A minimum recirculation valve fails to close (LPI-MOV-OO-F0610) are grouped into one super basic event, LPI-SYS-DEM-TRNA for LPI Train A fails on demand. Super basic event LPI-SYS-CF-DEM (LPI system common cause failures on demand) consists the following cut set basic events from the original or Stage 1 model:

- LPI-MDP-CF-START, Both LPI pumps A and B fail from common cause to start
- LPI-MOV-CF-F061011, Both LPI minimum circulation valves fail from common cause to close
- ESF-VCF-CF-TRNAB, Common cause failure of both trains of engineering safety features (ESF) actuation signals

230 A list of LPI super basic events is provided below:

- LPI-SYS-DEM-TRNA, LPI Train A fails on demand
- LPI-SYS-DEM-TRNB, LPI Train B fails on demand
- LPI-SYS-RUN-TRNA, LPI Train A fails to run
- LPI-SYS-RUN-TRNB, LPI Train B fails to run
- 235 • LPI-SYS-TM-TRNA, LPI Train A unavailable due to test or maintenance
- LPI-SYS-TM-TRNB, LPI Train B unavailable due to test or maintenance
- LPI-SYS-CF-DEM, LPI system common cause failures on demand
- LPI-SYS-CF-RUN, LPI system common cause failures to run
- NSW-SYS-TM-TRNA, NSW Train A unavailable due to test or maintenance
- 240 • NSW-SYS-TM-TRNB, NSW Train B unavailable due to test or maintenance
- NSW-SYS-CF-DEM, NSW system common cause failures on demand

245 Note that in order to further reduce the final number of basic events in Stage 2 model to be less than 20, NSW-SYS-TM-TRNA and NSW-SYS-TM-TRNB are removed from the model due to their low risk significance. Figure 7 presents the simplified Stage 2 LPI fault tree. Similarly, LPR-LL fault tree (and its subtrees) is simplified to include the following new super basic events, as well as some of the previous LPI super basic events:

- 250 • LPR-SYS-DEM-TRNA, LPR Train A fails on demand
- LPR-SYS-DEM-TRNB, LPR Train B fails on demand
- LPR-SYS-RUN-TRNA, LPR Train A fails to run
- LPR-SYS-RUN-TRNB, LPR Train B fails to run
- LPR-SYS-TM-TRNA, LPR Train A unavailable due to test or maintenance
- 255 • LPR-SYS-TM-TRNB, LPR Train B unavailable due to test or maintenance
- LPR-SYS-CF-DEM, LPR system common cause failures on demand
- LPR-SYS-CF-RUN, LPR system common cause failures to run
- 260 • LPR-XHE-XM-ERROR, Operator fails to initiate recirculation or hot leg recirculation

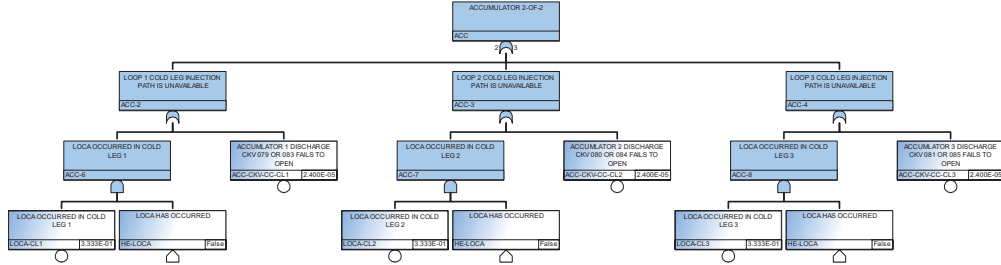


Figure 6: ACC FT stage2

Table 1: Accident Sequence Results for Original and Simplified LB-LOCA Models: CDF

Mode	Original Model		Stage 1 Model		Stage 2 Model	
	CDF	Cut Sets	CDF	Cut Sets	CDF	Cut Sets
LLOCA:2	1.82E-08	116	1.82E-08	116	1.82E-08	16
LLOCA:3	2.05E-09	52	2.05E-09	52	2.03E-09	10
LLOCA:4	1.20E-10	12	1.20E-10	12	1.20E-10	6
Total CDF	2.04E-08	180	2.04E-08	180	2.03E-08	32

Figure 8 presents the simplified Stage 2 LPR fault tree. Again, in order to reduce the final number of basic events in Stage 2 model to be less than 20, LPR-SYS-RUN-TRNA and LPR-SYS-RUN-TRNB are removed from the model due to their low risk significance.

#### 4.3. PRA Model Quantification Results

The simplified Stage 1 and Stage 2 LB-LOCA models are quantified in SAPHIRE with the same cutoff value of  $1E-12$ . As expected, Stage 1 model has exactly the same results with the original LB-LOCA model: same CDF value ( $2.04E-8/\text{year}$ ), same number of minimum cut sets, same number of basic events in minimum cut sets, and same risk significant basic events. Stage 2 model has a CDF of  $2.03E-8/\text{year}$  (less than 0.5% difference from the original model). The number of minimum cut sets is reduced from 180 to 32. The number of cut set basic events is reduced from 60 to 23. Excluding the initiating event (IE-LB-LOCA) and flag events (LOCA-CL1, LOCA-CL2, and LOCA-CL3), 19 basic events in Stage 2 model could be used in the RAVEN/RELAP5 simulation model as the manageable variables. Table 1 presents the quantification results for each accident sequence and the total CDF of LB-LOCA in the original, Stage 1, and Stage 2 models. The conditional core damage probabilities for the sequences are also obtained by quantifying the models with the LB-LOCA initiating event frequency is set to 1. Table 2 shows CCDP of accident sequences in the original, Stage 1, and Stage 2 LB-LOCA models. Table 3 shows the risk importance measure results for Stage 2 LB-LOCA model.

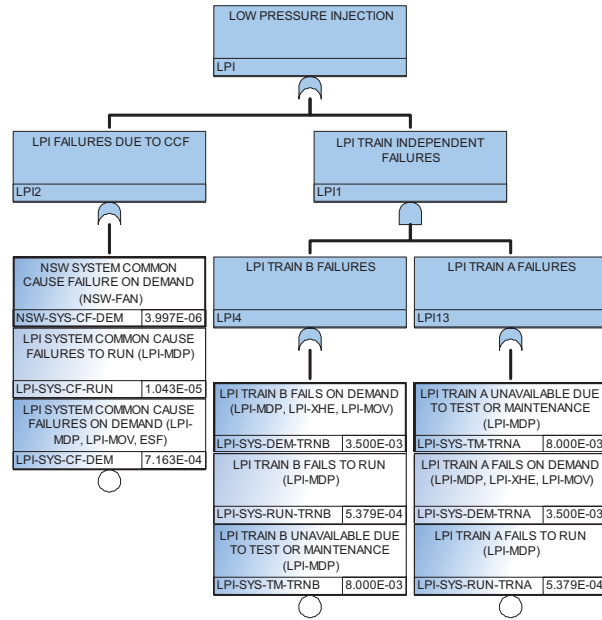


Figure 7: LPI FT stage2

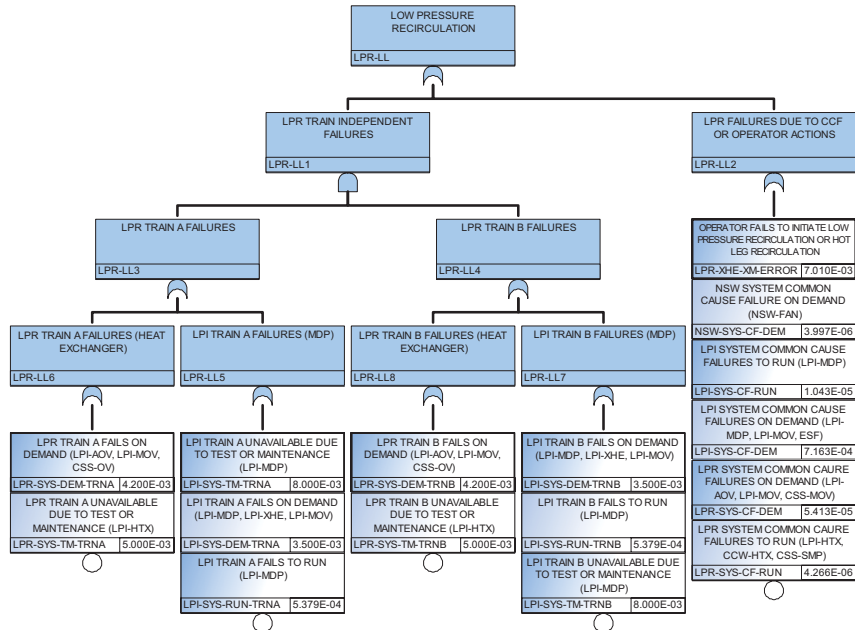


Figure 8: LPR FT stage2

Table 2: Accident Sequence Results for Original and Simplified LB-LOCA Models: CCDP

Mode	Original Model		Stage 1 Model		Stage 2 Model	
	CDF	Cut Sets	CDF	Cut Sets	CDF	Cut Sets
LLOCA:2	7.29E-03	3560	7.28E-03	173	7.27E-03	16
LLOCA:3	8.30E-04	2853	8.24E-04	61	8.12E-04	11
LLOCA:4	5.06E-05	44	4.80E-05	24	4.80E-05	9
Total CDF	8.17E-03	6457	8.15E-03	258	8.13E-03	36

Name	Probability	FV	RAW	Description
IE-LLOCA	2.50 E-6	1.00E+00	4.00E+05	LARGE LOCA
LPR-XHE-XM-ERROR	7.01 E-3	8.63E-01	1.23E+02	OPERATOR FAILS TO INITIATE LOW PRESSURE RECIRCULATION OR HOT LEG RECIRCULATION
LPI-SYS-CF-DEM	7.16 E-4	8.82E-02	1.23E+02	LPI SYSTEM COMMON CAUSE FAILURES ON DEMAND (LPI-MDP, LPI-MOV, ESF)
LPR-SYS-CF-DEM	5.41 E-5	6.67E-03	1.23E+02	LPR SYSTEM COMMON CAURE FAILURES ON DEMAND (LPI-AOV, LPI-MOV, CSS-MOV)
LPI-SYS-CF-RUN	1.04 E-5	1.29E-03	1.23E+02	LPI SYSTEM COMMON CAUSE FAILURES TO RUN (LPI-MDP)
LPR-SYS-CF-RUN	4.27 E-6	5.25E-04	1.23E+02	LPR SYSTEM COMMON CAURE FAILURES TO RUN (LPI-HTX, CCW-HTX, CSS-SMP)
NSW-SYS-CF-DEM	4.00 E-6	4.92E-04	1.23E+02	NSW SYSTEM COMMON CAUSE FAILURE ON DEMAND (NSW-FAN)
ACC-CKV-CC-CL1	2.40 E-5	1.97E-03	6.89E+01	ACCUMULATOR 1 DISCHARGE CKV 079 OR 083 FAILS TO OPEN
ACC-CKV-CC-CL2	2.40 E-5	1.97E-03	6.89E+01	ACCUMULATOR 2 DISCHARGE CKV 080 OR 084 FAILS TO OPEN
ACC-CKV-CC-CL3	2.40 E-5	1.97E-03	6.89E+01	ACCUMULATOR 3 DISCHARGE CKV 081 OR 085 FAILS TO OPEN

Table 3: Basic events with associated probability and RIMs values

Name	Probability	FV	RAW	Description
LPI-SYS-DEM-TRNA	3.50 E-3	9.15E-03	3.57E+00	LPI TRAIN A FAILS ON DEMAND (LPI-MDP, LPI-XHE, LPI-MOV)
LPI-SYS-DEM-TRNB	3.50 E-3	9.15E-03	3.57E+00	LPI TRAIN B FAILS ON DEMAND (LPI-MDP, LPI-XHE, LPI-MOV)
LPR-SYS-DEM-TRNA	4.20 E-3	1.10E-02	3.56E+00	LPR TRAIN A FAILS ON DEMAND (LPI-AOV, LPI-MOV, CSS-OV)
LPR-SYS-DEM-TRNB	4.20 E-3	1.10E-02	3.56E+00	LPR TRAIN B FAILS ON DEMAND (LPI-AOV, LPI-MOV, CSS-OV)
LPI-SYS-RUN-TRNA	5.38 E-4	1.37E-03	3.51E+00	LPI TRAIN A FAILS TO RUN (LPI-MDP)
LPI-SYS-RUN-TRNB	5.38 E-4	1.37E-03	3.51E+00	LPI TRAIN B FAILS TO RUN (LPI-MDP)
LPI-SYS-TM-TRNA	8.00 E-3	8.12E-03	2.00E+00	LPI TRAIN A UNAVAILABLE DUE TO TEST OR MAINTENANCE (LPI-MDP)
LPI-SYS-TM-TRNB	8.00 E-3	8.12E-03	2.00E+00	LPI TRAIN B UNAVAILABLE DUE TO TEST OR MAINTENANCE (LPI-MDP)
LPR-SYS-TM-TRNA	5.00 E-3	5.07E-03	2.00E+00	LPR TRAIN A UNAVAILABLE DUE TO TEST OR MAINTENANCE (LPI-HTX)
LPR-SYS-TM-TRNB	5.00 E-3	5.07E-03	2.00E+00	LPR TRAIN B UNAVAILABLE DUE TO TEST OR MAINTENANCE (LPI-HTX)

Table 3: Basic events with associated probability and RIMs values (continued)

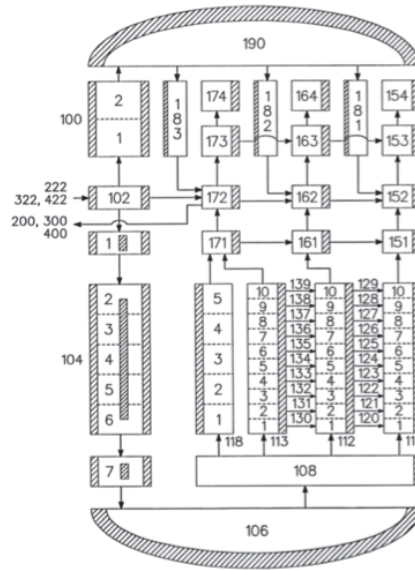


Figure 9: RELAP5-3D RPV Model.

## 5. PWR Deterministic Modelling

285 SAPHIRE code Standardized Plan Analysis Risk (SPAR) used for static PRA analysis is based on a generic 3-loops Westinghouse PWR model. Dynamic PRA calculations were executed by RELAP5-3D/RAVEN, so a RELAP5-3D system code model for a generic 3-loops Westinghouse PWR has been developed. The description of this model is reported hereafter.

### 290 5.1. RELAP5-3D Model for 3 Loops PWR

The RELAP5-3D model is based on the so-called INL Generic PWR (IG-PWR) model used for calculations of different LWRS/RISMC tasks. The RELAP5-3D input deck is modeling a 2.5 GWth Westinghouse 3-loops PWR, including the reactor pressure vessel (RPV), the 3 loops and the primary and secondary sides of the steam generators (SG) (see Figure 9 and Figure 10).

295 Four independent channels are used for representing the reactor core. Three channels model the active core and one channel models the core bypass. Different power values are assigned to the three core channels in order to take into account the radial power distribution. Passive and active heat structures simulate the heat transfer between the coolant and fuel, the structures and the secondary side of the IGPWR.

300 Table 4 reports the steady state values obtained for the RELAP5-3D model and the comparison with reference values, showing that the agreement is good.

305 For the transient calculation, a horizontal LBLOCA on the cold-leg RPV nozzle was considered. The break was supposed to happen on the pressurizer

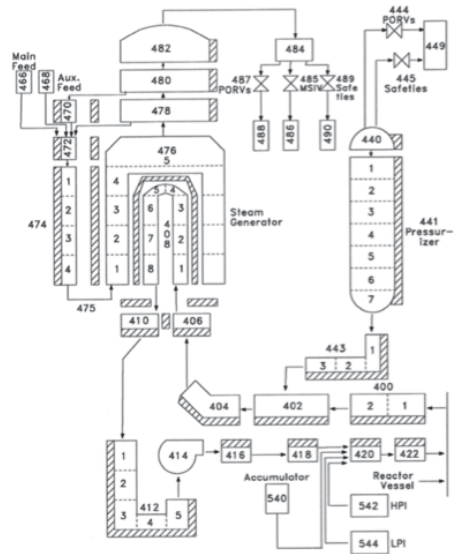


Figure 10: RELAP5-3D MCC and SG Model.

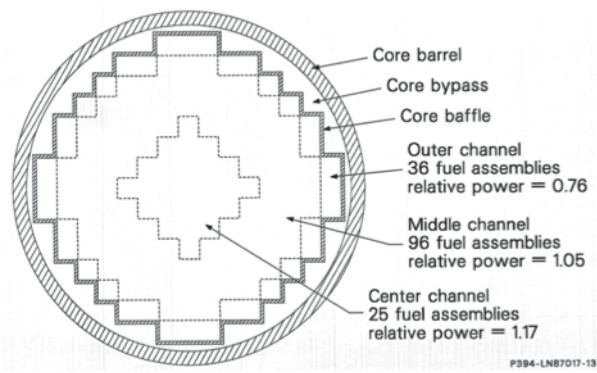


Figure 11: RELAP5-3D Core Model.



Parameter	Reference value	RELAP5-3D value	Deviation (%)
Reactor Power (W)	2,546	2,546	imposed
PRZ Pressure (MPa)	15.5	15.57	imposed
Total RCS Coolant Loop Flowrate (Kg/s)	12,738	12,738	0.0
CL Temperature (K)	555.6	557.3	0.3
HL Temperature (K)	591.8	593.1	0.2
Feed-water Temperature (K)	501.5	501.5	imposed
Steam Flowrate per SG1 (K)	473.	470.1	-0.6
Steam Flowrate per SG2 (K)	473.	470.7	-0.5
Steam Flowrate per SG3 (K)	473.	471.0	-0.4
Steam Pressure at the Outlet Nozzle (MPa)	5.405	5.405	imposed
Liquid Mass per SG (Kg)	41,639	41,640	0.0
Steam Temperature (K)	542	542	0.0

Table 4: RELAP5-3D LBLOCA steady state values.

loop. Several LBLOCA cases were run, including some considered by Westinghouse for LBLOCA spectrum analysis (U.S. NRC 2011):

- 2A, Double-Ended Guillotine Break (DEGB);
- 1A;
- 310 • 10 inches diameter;
- 8 inches diameter;
- 6 inches diameter.

For the LBLOCA DEGB, the total break area was  $2 \times 0.383 \text{ m}^2$  ( $2 \times 4.125 \text{ ft}^2$ ), corresponding to a 0.7 m (27.56 inches) diameter pipe. The RELAP5-3D model of the break is reported in Figure 12.

For the other 4 cases, the total break area was:

- case 1A:  $0.383 \text{ m}^2$  ( $4.125 \text{ ft}^2$ ), or 0.7 m (27.5 inches) diameter break;
- case 10 inches:  $0.0506 \text{ m}^2$  ( $0.545 \text{ ft}^2$ ), or 0.254 m (10 inches) diameter break;
- 320 • case 8 inches:  $0.0324 \text{ m}^2$  ( $0.349 \text{ ft}^2$ ), or 0.203 m (8 inches) diameter break;
- case 6 inches:  $0.0182 \text{ m}^2$  ( $0.196 \text{ ft}^2$ ), or 0.152 m (6 inches) diameter break.

The scheme of the break is reported in Figure 5.

The Emergency Core Cooling Injection System (ECCS) model is based on the information provided by (U.S. NRC 2011), (NRC 2013), (Dominion 2007). The main characteristics of it are reported in Table 5, Table 6 and Table 7.

The actuation signals for the ECCS and the containment sprays are reported in Table 8.

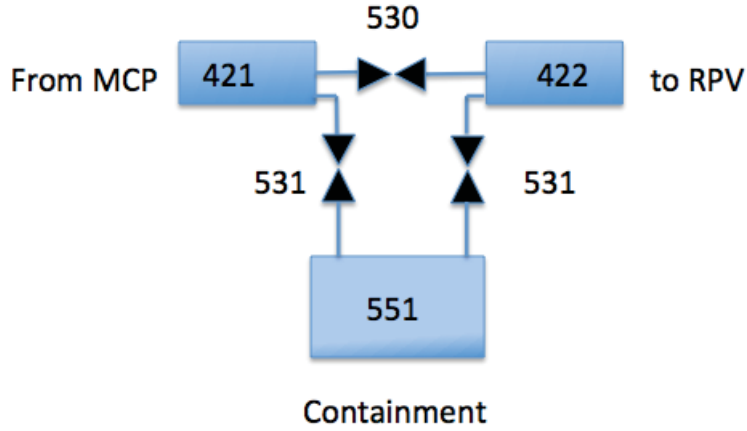


Figure 12: RELAP5-3D LBLOCA DEGB model scheme.

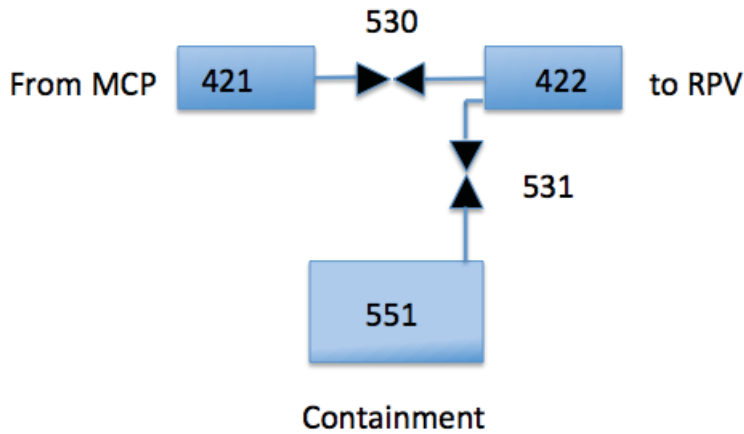


Figure 13: RELAP5-3D LBLOCA 1A/10-8-6 inches model scheme.

Table 5: RELAP5-3D ECCS main parameters.

ECCS Parameters	Value (SI)	Value (Imperial)
Accumulator Water Volume [m <sup>3</sup> / ft <sup>3</sup> ]	3 x 28.32	3 x 1000
Accumulator Gas Pressure [MPa / psig]	4.00	580
Accumulator Water Temperature [C / F]	40.6	105.0
HPI volumetric flow [m <sup>3</sup> /s / gpm]	3 x 0.0708 (at 1,767 m)	3 x 150 (at 5,800 ft)
HPI design head [MPa / psi]	17.34	2515.3
LPI volumetric flow [m <sup>3</sup> /s / gpm]	2 x 1.416 (at 68.6 m)	2 x 3,0007 (at 225 ft)
LPI design head [MPa / psi]	6.728	97.58

Table 6: RWST main parameters.

Parameters	Value (SI)	Value (Imperial)
Max Water Volume [m <sup>3</sup> / gal]	1514.2	400,000
Required Minimum Water Volume [m <sup>3</sup> / gal]	1465.3	387,000
Minimum Water Volume [m <sup>3</sup> / gal]	53.0	14,000
Water Temperature [C / F]	7.2	45.0
RWST / Containment sump switch time (s)	150.0	

Table 7: Containment main parameters.

Parameters	Value (SI)	Value (Imperial)
Volume [m <sup>3</sup> / ft <sup>3</sup> ]	49,000	1,730,000
Design Pressure [MPa / psig]	0.31	45
Operating Pressure [MPa / psia]	0.062 to 0.071	9 to 10.3
Operating Temperature [C / F]	24 to 52	75 to 125
Containment sprays mass flow [m <sup>3</sup> /s / gpm]	2 x 0.183	2 x 2900

Table 8: ECCS and Containment Spray actuation signals.

Parameters	Value (SI)	Value (Imperial)
Low pressure signal in PRZ [MPa/psig]	< 12.3	< 1789.7
Low-low pressure signal in PRZ [MPa/psig]	< 12.2	< 1775.
High Containment Pressure [MPa/psia]	> 0.122	> 17.7
High Steamline Delta Pressure [MPa/psid]	> 0.827	> 120.
Spray signal for Containment Pressure [MPa/psig]	> 0.172	> 25
Spray OFF for Containment Pressure [MPa/psig]	< 0.082	< 12

The operators and the emergency crew actions were limited to few actions. The initial ECCS and containment sprays actuations were supposed to be automatically performed by the reactor protection system.

## 6. PWR Stochastic Modeling

In the Dynamic PRA analysis, the stochastic modeling of the PWR system have been performed for two different cases:

- Case 1: set of RAVEN stochastic variables coincide with the set of macro basic events defined in Section 4
- Case 2: set of RAVEN stochastic variables include not only the set of macro basic events defined in Section 4 but also includes time related variables. As an example, the failure to run of a component is modeled quantitatively by sampling not only if such event occurs but the failure time of such component is actually sampled.

In Case 1, the PWR models in both Dynamic and classical PRA methods are identical: there is a one-to-one connection between the stochastic elements (basic events vs. sampled variables) and accident progression (system simulator vs. ET) of both methods.

In case 1 the set of macro basic events coincide with the set of stochastic parameters sampled by RAVEN. While in SAPHIRE each macro basic event ( $BE_i$ ) is characterized by probability value ( $p_i$ ), in RAVEN its corresponding stochastic variable ( $v_i$ ) is modeled through a Bernoulli distribution  $v_i \sim \text{Bern}(p_i)$ . From this analysis we expect very similar results since the capabilities of Dynamic PRA methods are not exploited. However, this is a first test toward benchmarking Dynamic vs. classical PRA methods in order to understand modeling differences and impact on final results.

## 7. Dynamic PRA Analysis

The Dynamic PRA analysis have been performed using RAVEN and RELAP5-3D and employing both desktop and High Performing Computing (HPC) systems.

Case 1 has been performed by following these steps:

1. Perform the set of RAVEN/RELAP5-3D calculations. The variables of interests are the following
  - ACC\_1: Accumulator 1 failure
  - ACC\_2: Accumulator 2 failure
  - LPI\_A: LPI train A failure
  - LPI\_B: LPI train B failure
  - LPR\_A: LPR train A failure

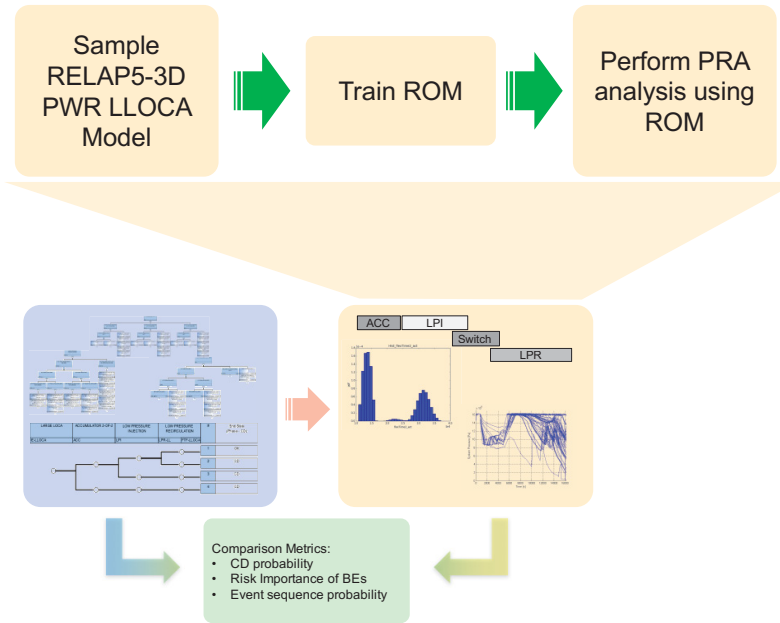


Figure 14: RAVEN/RELAP5-3D workflow overview.

- LPR\_B: LPR train A failure

Since these variables are discrete in nature (i.e., 0 or 1) we have explored all possible combinations (using a Grid sampling strategy), i.e.,  $2^6 = 64$ , by simulating using RELAP5-3D the system response for all 64 cases.

2. Use the data generated in Step 1 to train a ROM. The ROM predict system outcome (OK or CD) and maximum clad temperature given a combination of the six input variables listed above
3. Perform a RAVEN analysis using the ROM determined in Step 2. The set of input variables are the ones listed in Table 3: the 18 macro basic events defined also in the SAPHIRE LLOCA ET/FT model. In order to create a connection between the 18 sampled variables and the 6 input variables of the ROM, a set of six RAVEN functions have been introduced in the analysis so that, for each combination of the 18 sampled variables, the corresponding combination of the six ROM input variables is determined. Since the sampled variables are discrete in nature (True or False, 0 or 1), all possible combinations (i.e.,  $2^{18} = 262,144$ ) of the sampled variables have been simulated (using a Grid sampling strategy). Note that the outcome of each combination is determined by evaluating the ROM instead of RELAP5-3D and, thus, computational time is strongly reduced.
4. Process the data generated in Step 3 and determine CD probability along with the risk measure for each sampled variable.

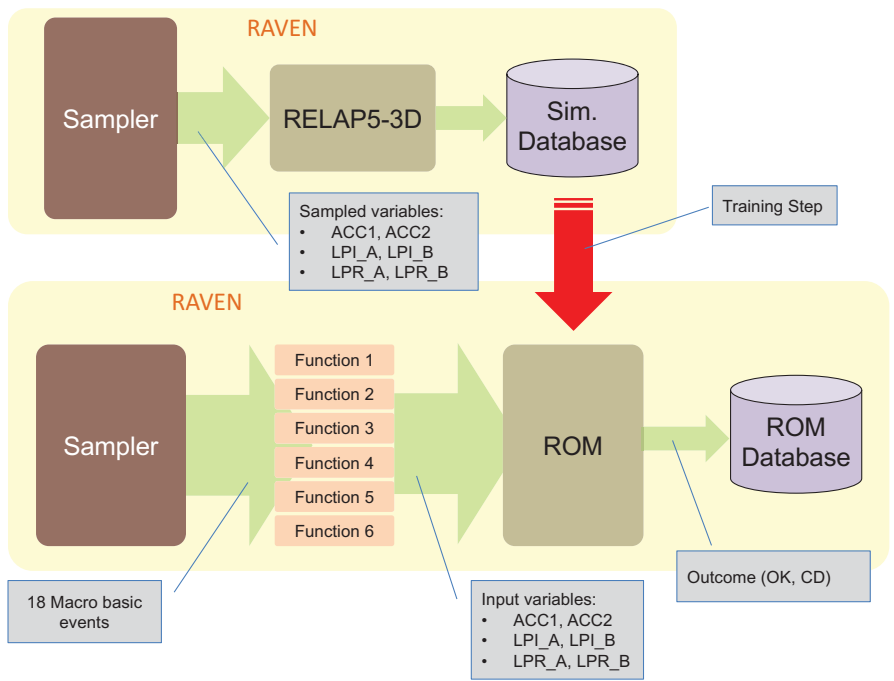


Figure 15: Detailed workflow of RAVEN/RELAP5-3D analysis.

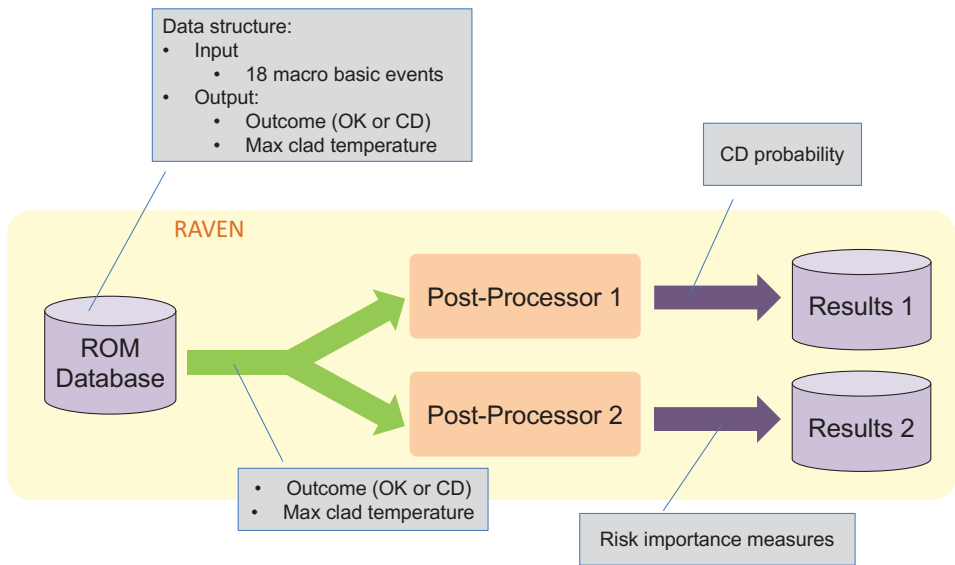


Figure 16: Data analysis of RAVEN/RELAP5-3D data sets.

Table 9: Comparison of results: analysis of  $P_{CD}$

	SAPHIRE	RAVEN
$P_{CD}$	8.13 E-3	8.24 E-3

## 8. Comparison of Results

The comparison between the two PRA analyses has been performed on three different steps by considering:

1. CD probability
- 390 2. Probability associated to each accident progression sequence
3. Importance measure (FV and RAW) associate to each macro basic event

Note how the three steps have an increasing level of detail from coarse (i.e., first step) to very fine (i.e., importance measures). This approach allows us to progressively measure the differences between classical and Dynamic PRA methods.

395 Regarding the first step, the comparison of  $P_{CD}$  shows very similar results as shown in Table 9. Hence, as first conclusion it can be stated that the accident progression has been modeled in a fairly identical way.

400 The next analysis step has focused on the set of accident progression sequences generated by SAPHIRE in and ET form and the ones generated by RAVEN/RELAP5-3D in the form of simulated transients. This has been performed by associating each transient simulated by RAVEN/RELAP5-3D to a specific branch of the LOCA ET as follows:

- 405 • identify the ET branching conditions in the transient temporal evolution (e.g., successful activation of the accumulator system)
- determine the successful/unsuccessful outcome of each branching condition
- identify the ET branch that matches the set of branching condition outcomes; if not match is found then the ET requires a review (e.g., additional branches/branching conditions)
- 410

Figure 17 shows a summary of this analysis where, for each ET branch, the corresponding branch probability has been calculated using SAPHIRE and RAVEN/RELAP5-3D. The major difference in this analysis is located in the probability associated to branch 4

### 415 8.1. Consistency check SAPHIRE vs. RAVEN-RELAP5-3D models

Since all the investigated cases were LBLOCA, a combination of ACCs and LPIS was activated at each RELAP5-3D run. In order to determine if the acceptance criteria used by the SAPHIRE model were consistent with the ones derived by RELAP5-3D/RAVEN, several reference LB-LOCA calculations were

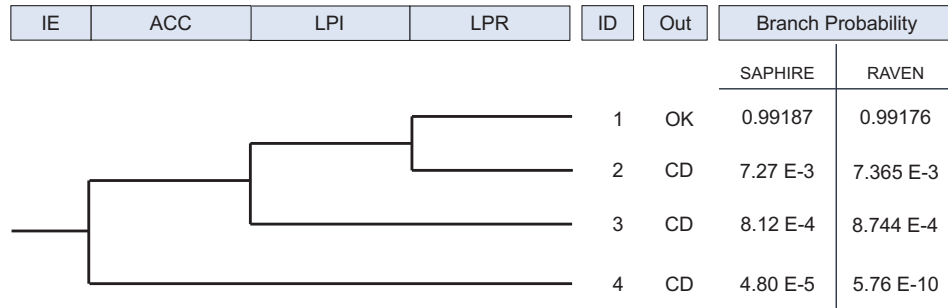


Figure 17: ET branch probabilities comparison.

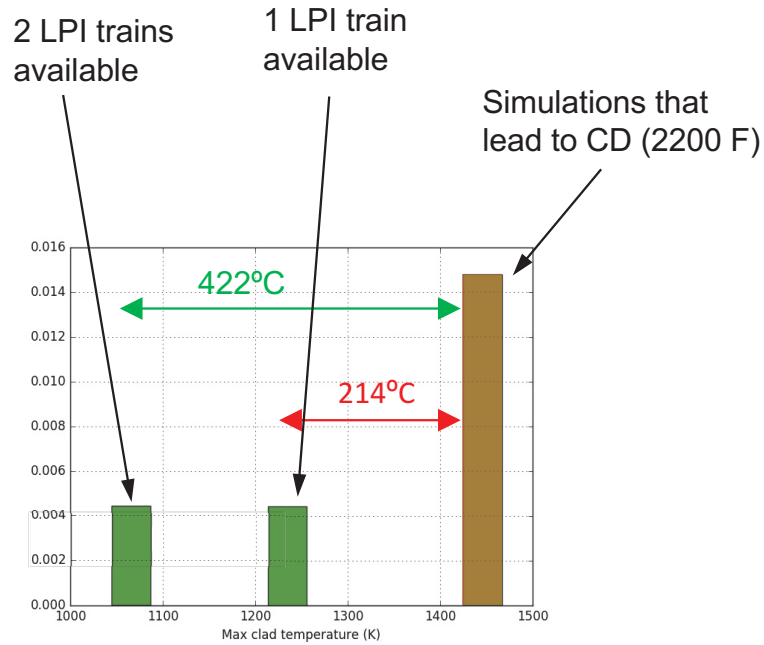


Figure 18: Histogram of PCT for branch 4 (RAVEN/RELAP5 case)



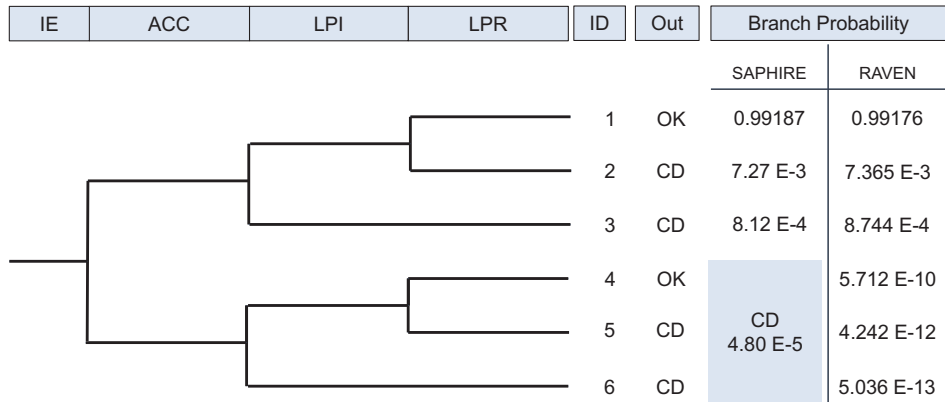


Figure 19: Update ET structure given RAVEN/RELAP5 data.

Table 10: Comparison of results.

BE	SAPHIRE		RAVEN	
	FV	RAW	FV	RAW
IE-LLOCA	1.	4.00 E+5	1.	4.00 E+5
LPR-XHE-XM-ERROR	8.63 E-1	123	8.50	121
LPI-SYS-CF-DEM	8.82 E-2	123	8.62 E-2	121
LPR-SYS-CF-DEM	6.67 E-3	123	1.25 E-3	121
LPI-SYS-CF-RUN	1.29 E-3	123	1.25 E-3	121
LPR-SYS-CF-RUN	5.25 E-3	123	1.25 E-3	121
NSW-SYS-CF-DEM	4.92 E-4	123	4.8 E-4	121
ACC-CKV-CC-CL1	1.97 E-3	68.9	0.	1.
ACC-CKV-CC-CL2	1.97 E-3	68.9	0.	1.
ACC-CKV-CC-CL3	1.97 E-3	68.9	0.	1.
LPI-SYS-DEM-TRNA	9.15 E-3	3.57	8.72 E-3	3.48
LPI-SYS-DEM-TRNB	9.15 E-3	3.57	8.72 E-3	3.48
LPR-SYS-DEM-TRNA	1.10 E-2	3.56	1.04 E-2	3.48
LPR-SYS-DEM-TRNB	1.10 E-2	3.56	1.04 E-2	3.48
LPI-SYS-RUN-TRNA	1.37 E-3	3.51	1.33 E-3	3.48
LPI-SYS-RUN-TRNB	1.37 E-3	3.51	1.33 E-3	3.48
LPI-SYS-TM-TRNA	8.12 E-3	2.00	2.0 E-2	3.48
LPI-SYS-TM-TRNB	8.12 E-3	2.00	2.0 E-2	3.48
LPR-SYS-TM-TRNA	5.07 E-3	2.00	1.24 E-2	3.48
LPR-SYS-TM-TRNB	5.07 E-3	2.00	1.24 E-2	3.48

Table 11: LBLOCA DEGB results

ACCs	LPIS	1st PCT (K)	2nd PCT (K)	1st Margin	2nd Margin
0	1	1044.9	1218.8	432.1	258.2
1	1	1044.9	1002.2	432.1	474.8
2	1	1044.9	913.1	432.1	563.9
0	2	1044.9	1084.5	432.1	392.5
1	2	1044.9	958.1	432.1	518.9
2	2	1044.9	904.6	432.1	572.4

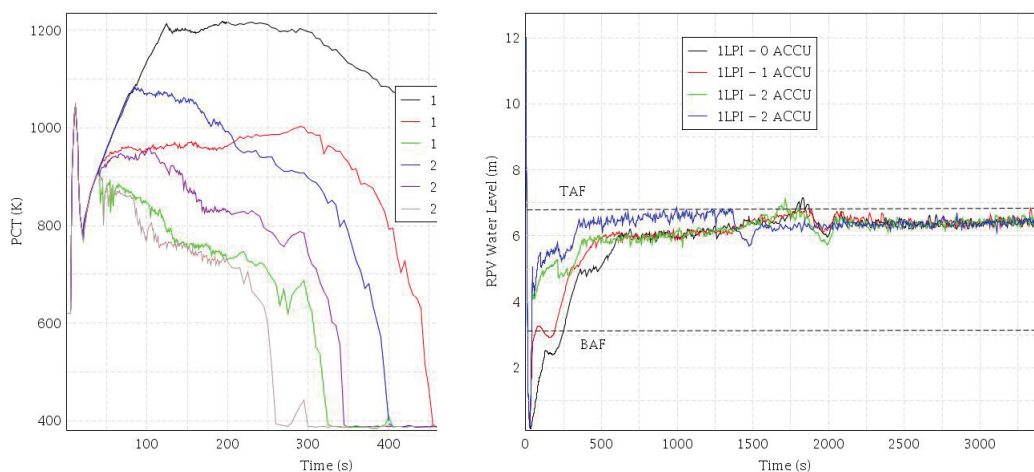


Figure 20: LBLOCA DEGB cases. PCT (left), RPV level (right).

420 performed, changing at each run the actuation time and the availability of the  
 ECCS components.

Results from the set of LB-LOCA-DEGB calculations are reported in Table 11.

425 The trend of the RPV water level and the PCT for the transients reported  
 in Table 6 are show in Figure 20. No core damage conditions (PCT<sub>i</sub>2200 F or  
 1477 K) were found for the investigated cases.

The trends of the RPV water level and the PCT for the transients are show  
 in Figure 21. No core damage condition (PCT<sub>i</sub>2200 F) was found for the investigated  
 cases.

430 The RELAP5-3D analyses demonstrated that the acceptance criterion for  
 LBLOCA is the availability of at least one LPIS pump. Instead the SAPHIRE  
 SPAR model success criterion for LB-LOCA requires the availability of at least  
 one LPIS pump and one accumulator.

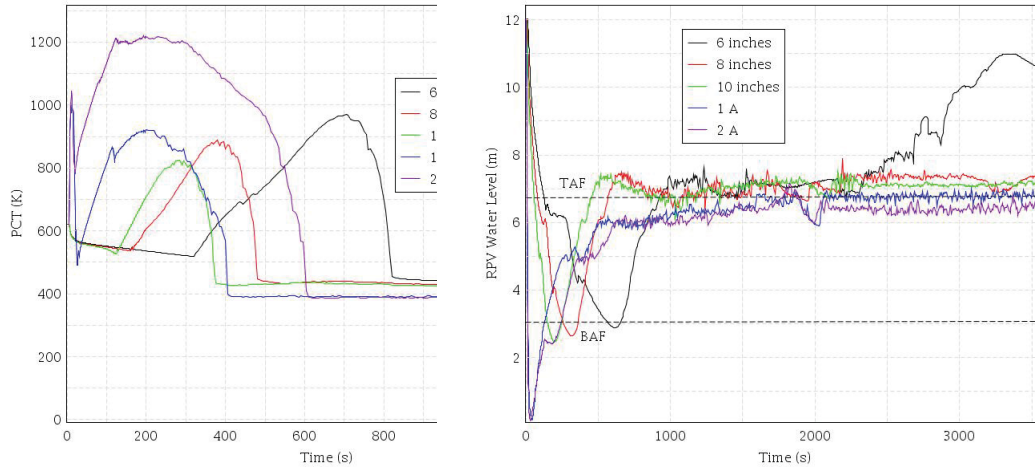


Figure 21: LBLOCA DEGB cases. PCT (left), RPV level (right).

## 9. Conclusions

435 In this paper we have investigated a detailed comparison between Classical  
and Dynamic PRA methods. The considered system has been a 3-loop PWR  
under an LB-LOCA initiating event. We have used several metrics to quantify  
this comparison ranging from CD probability to event sequence probabilities and  
basic event risk importance measures. We have described the process of compar-  
440 ison and how the model data has been shared between the PRA approaches. The  
outcome of the comparison highlighted limitations of classical PRA methods in  
terms of modeling accident sequences due to conservative modeling assumptions  
and success criteria.

## References

- 445 [1] R. C. D. Team, RELAP5-3D Code Manual, Technical Report, Idaho Na-  
tional Laboratory Technical Report, 2005.
- [2] R. O. Gauntt, MELCOR Computer Code Manual, Version 1.8.5, Vol. 2,  
Rev. 2, Sandia National Laboratories, NUREG/CR-6119, 2000.
- [3] EPRI, Modular Accident Analysis Program 5 (MAAP5) Applications Guid-  
450 ance: Desktop Reference for Using MAAP5 Software - Phase 2 Report,  
Technical Report, Electric Power Reserach Institute, Palo Alto (CA), 2013.
- [4] C. Rabiti, A. Alfonsi, J. Cogliati, D. Mandelli, R. Kinoshita, RAVEN, a  
new software for dynamic risk analysis, in: Proceedings of the Probabilistic  
Safety Assessment andnd Management (PSAM) 12, 2014.

- 455 [5] B. Rutt, U. Catalyurek, A. Hakobyan, K. Metzroth, T. Aldemir, R. Denning, S. Dunagan, D. Kunsman, Distributed dynamic event tree generation for reliability and risk assessment, in: 2006 IEEE Challenges of Large Applications in Distributed Environments, 2006, pp. 61–70.
- 460 [6] E. Hofer, M. Kloos, B. Krzykacz-Hausmann, J. Peschke, M. Woltereck, An approximate epistemic uncertainty analysis approach in the presence of epistemic and aleatory uncertainties, *Reliability Engineering & System Safety* 77 (2002) 229–238.
- 465 [7] K. S. Hsueh, A. Mosleh, The development and application of the accident dynamic simulator for dynamic probabilistic risk assessment of nuclear power plants, *Reliability Engineering & System Safety* 52 (1996) 297–314.
- [8] J. Devooght, C. Smidts, Probabilistic dynamics as a tool for dynamic PSA, *Reliability Engineering & System Safety* 52 (1996) 185 – 196.
- 470 [9] D. Mandelli, Z. Ma, C. Parisi, D. Maljovec, A. Alfonsi, C. Smith, Measuring risk-importance in a simulation-based pra framework - part i: Mathematical framework, Draft for *Reliability Engineering & System Safety* (2017).
- [10] C. Smith, J. Knudsen, D. ONeal, T. Peterson, K. Vedros, SAPHIRE 8 New Features and Capabilities, Technical Report, Idaho National Laboratory Technical Report: INL/EXT-08-14841, 2008.
- 475 [11] E. P. R. Institute, Computer Aided Fault Tree Analysis System (CAFTA), Version 6.0b, Technical Report, Electric Power Research Institute, 2014.